



Cite this: *Med. Chem. Commun.*,  
2018, 9, 795

## Design, synthesis and biological evaluation of novel 1,3-diarylpyrazoles as cyclooxygenase inhibitors, antiplatelet and anticancer agents†

Nazan Incel, <sup>a</sup> Yesim Ozkan, <sup>b</sup> Nilufer Nermin Turan, <sup>c</sup> Deniz Cansen Kahraman, <sup>d</sup> Rengul Cetin-Atalay <sup>d</sup> and Sultan Nacak Baytas <sup>id</sup> <sup>\*a</sup>

With the aim of achieving new compounds possessing both anti-inflammatory and antiplatelet activities, we synthesized (*E*)-3-[3-(pyridin-3/4-yl)-1-(phenyl/sulfonylmethylphenyl)-1*H*-pyrazol-4-yl]acrylamides, and evaluated their COX-1 and COX-2 inhibitory and antiplatelet activities. Since COX-2 inhibitory and antiplatelet compounds have anticancer potential, we also screened their antiproliferative effects against three human cancer cell lines. Compounds **5n**, **5p**, **5s**, **10d**, **10g** and **10i** were determined as dual COX-2 inhibitor/antiplatelet compounds. Compound **10h** appeared to be a compound that exhibited antiplatelet activity without inhibiting the COX enzyme. Compounds **5h**, **10a** and **10i** were the most effective derivatives which displayed antiproliferative activity against Huh7, MCF7 and HCT116 cells. Particularly, compound **10i**, as the compound exhibiting the highest cytotoxic, antiplatelet and COX-2 inhibitory activity, was remarkable.

Received 12th January 2018,  
Accepted 16th March 2018

DOI: 10.1039/c8md00022k

rsc.li/medchemcomm

### Introduction

Studies towards better tolerated and potent non-steroidal anti-inflammatory drugs (NSAIDs) with fewer side effects as compared to current NSAIDs have been of interest for many years. The non-selective inhibition of the two isoforms of COX is thought to be responsible for the gastric side effects associated with the chronic use of NSAIDs. It was thought that more selective COX-2 inhibitors would have reduced side effects.<sup>1,2</sup> Recently, research has focused on the development of COX-2-selective inhibitors, which are demonstrated to possess significantly enhanced gastric safety compared to non-selective NSAIDs. Celecoxib and rofecoxib are two well-known selective COX-2 inhibitors belonging to the COXIB class. However, rofecoxib and other COX-2 inhibitors have been withdrawn from the market due to their adverse cardiovascular side effects.<sup>3–7</sup> While a selective COX-2 inhibitor causes the reduction of the prostacyclin (PGI<sub>2</sub>) amount, thromboxane A<sub>2</sub>

(TXA<sub>2</sub>) production is still continued in platelets by the COX-1 isoform.<sup>8</sup>

TXA<sub>2</sub> is a cellular lipidic mediator resulting from metabolism of arachidonic acid (AA) by cyclooxygenases and thromboxane synthase<sup>9</sup> and produced by platelets, macrophages and lung parenchyma.<sup>10</sup> TXA<sub>2</sub> is a potent vasoconstrictor as well as a labile platelet aggregation inducer. Conversely, PGI<sub>2</sub> is synthesized in the walls of the vasculature and inhibits thrombus formation. It is thought that the cardiovascular toxicity of coxibs was generated because of the imbalance between PGI<sub>2</sub> and TXA<sub>2</sub> levels.<sup>11</sup> In a patient who requires effective anti-inflammatory treatment and has a high risk for both gastrointestinal bleeding and cardiovascular thrombosis, the use of selective COX-2 inhibitors with antiplatelet agents like thromboxane synthase inhibitors (TxSI) is being recommended.<sup>12,13</sup> This aspect has encouraged the search for dual inhibitors of both COX-2 and thromboxane synthase (TxS) which should display an enhanced anti-inflammatory potency with fewer side effects. Compared to COX or TxS pathways as single inhibitors, dual inhibitors shall present at least two major advantages: first, dual inhibitors, by acting on the AA metabolic pathway, possess a wide range of anti-inflammatory activities; second, dual inhibitors appear to be almost exempt from gastric and cardiac toxicity, which are the most troublesome side effects of COX inhibitors.<sup>14</sup>

There are several reviews which are mainly focused on the molecular and functional bases of the inhibition of COX enzymes by non-selective and COX-2-selective inhibitors.<sup>15,16</sup> The pharmacophore for most of the selective COX-2

<sup>a</sup> Division of Pharmaceutical Sciences, Department of Pharmaceutical Chemistry, Faculty of Pharmacy, Gazi University, 06330, Ankara, Turkey.

E-mail: baytas@gazi.edu.tr; Fax: +90 (312) 223 5018

<sup>b</sup> Department of Biochemistry, Faculty of Pharmacy, Gazi University, 06330, Ankara, Turkey

<sup>c</sup> Department of Pharmacology, Faculty of Pharmacy, Gazi University, 06330, Ankara, Turkey

<sup>d</sup> Cancer Systems Biology Laboratory, Graduate School of Informatics, METU, 06800, Ankara, Turkey

† Electronic supplementary information (ESI) available. See DOI: 10.1039/c8md00022k

inhibitors consists of a central 1,2-diaryl-substituted five-membered heterocyclic ring.<sup>2,17-19</sup> Some 1,3-diarylpyrazole derivatives have also been reported as selective COX-2 inhibitors.<sup>20,21</sup> The essential structural features of TXA<sub>2</sub> synthase inhibitors are a basic nitrogen atom of a substituted pyridine or imidazole ring and a carboxylic acid group separated by an unsaturated *trans*-alkyl chain.<sup>11</sup> It is found that there should be an appropriate length between the nitrogen atom of the pyridine residue, which is known to selectively inhibit TXA<sub>2</sub> synthase *via* chelating with iron, and the carboxylic acid moiety for selective TxSI.<sup>22,23</sup>

It is widely recognized that inflammation may trigger cancer initiation and progression. COX-2 is overexpressed in most solid tumors.<sup>24-27</sup> COX-2 has been recognized as an important molecule promoting tumor progression and angiogenesis. Due to the activities of COX pro-inflammatory metabolites, this enzyme is a relevant target for anticancer therapies.<sup>28</sup> COX-2 inhibitors have anticancer effects which include inducing apoptosis, suppressing proliferation, reducing angiogenesis and weakening invasiveness.<sup>29,30</sup>

Platelets play major roles in cancer progression by providing surface and granular contents for several interactions as well as behaving like immune cells.<sup>31,32</sup> Therefore, the anticancer potential of antiplatelet therapy has been intensively investigated for many years.<sup>33,34</sup> Anti-platelet agents may prevent cancer and decrease tumor growth and metastatic potential, as well as improve the survival of cancer patients. Advanced knowledge about the molecular and functional aspects of platelet-mediated tumor dissemination motivated scientists to search for drugs with anticancer potential.<sup>28</sup>

Our research includes the design, synthesis, and analgesic, anti-inflammatory, antiplatelet and anticancer screening of bioactive compounds.<sup>35-40</sup> In our previous work,<sup>41</sup> a series of (*E*)-3-[3-(2,3-dihydro-3-methyl-2-oxo-3*H*-benzoxazol-6-yl)-1-phenyl-1*H*-pyrazol-4-yl]acrylamides **1** (Fig. 1) has been

synthesized using both conventional and microwave-assisted methods and evaluated for their *in vitro* inhibitory activities on COX-1 and COX-2 isoforms using human whole blood assay as well as their antiplatelet profiles against human platelet aggregation using arachidonic acid, as agonists. (*E*)-3-[3-(Pyridin-4-yl)-1-phenyl-1*H*-pyrazol-4-yl]acrylamides **2** were also synthesized and evaluated as inhibitors of AA-induced and collagen-induced platelet aggregation with a focus on the role of the pyridine replacement of one of the aryl groups in the diarylpyrazole template.<sup>42</sup>

In our other works, a series of novel thiophene-containing 1,3-diarylpyrazole derivatives and ester and amide derivatives of pyridine-containing 1,3-diarylpyrazoles were synthesized and their anticancer activities against MCF7, MDA-MB-231, HeLa, Raji and HL60 human cancer cell growth were investigated by MTT assay. Derivative **3** bearing a benzylpiperidine group at the amide portion in the thiophene-containing 1,3-diarylpyrazole series showed significant inhibitory effects against the Raji and HL60 cell lines.<sup>43</sup> In the series of ester and amide derivatives of 1,3-diarylpyrazoles, two derivatives were found as the most promising anticancer agents in Raji cells.<sup>44</sup> In another study, we synthesized a series of pyrazolic chalcone derivatives **4** and evaluated their anti-proliferative activities in comparison with clinically used chemotherapeutics such as 5-FU and cladribine against human cancer cell lines. Among the tested compounds, four derivatives bearing a 3/4-pyridyl moiety at the C(3)-position of the central pyrazole ring were the most effective derivatives, which displayed anti-proliferative activity with IC<sub>50</sub> values smaller than 5 μM against HCC cells. Moreover, these compounds were less active on transformed and normal cells (MCF12A and MRC-5). We showed that two derivatives in these series caused cell cycle arrest at the G2/M phase, induced apoptotic cell death and decreased the levels of phospho-cyclin B1 at the Ser147 residue.<sup>45</sup>

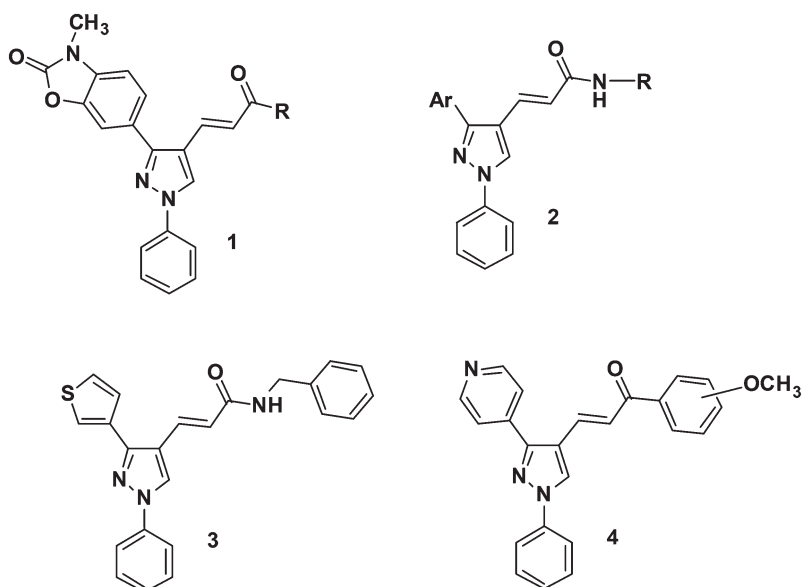


Fig. 1 Bioactive compounds belonging to our chemical library.

In continuation of our previous works, we describe herein the design, synthesis, and COX-1 and COX-2 inhibitory, antiplatelet and anticancer activities of new (*E*)-3-[3-(pyridin-3/4-yl)-1-(phenyl/sulfonylmethylphenyl)-1*H*-pyrazol-4-yl]-acrylamides, bearing a central pyrazole ring substituted with phenyl, pyridine and 3-oxoprop-1-en-1-yl fragments at 1, 3 and 4 positions, respectively (Fig. 2).

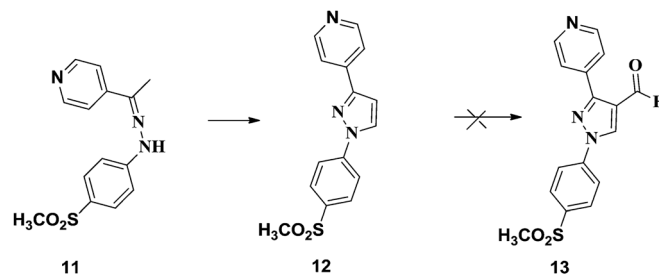
## Results and discussion

### Chemistry

The synthesis of (*E*)-3-[1-phenyl-3-(pyridin-3/4-yl)-1*H*-pyrazol-4-yl]acrylamides has been accomplished as outlined in Scheme 1. Firstly, the hydrazone derivatives **2** were generated by carrying out condensation in the presence of an appropriate acetylpyridine derivative, phenylhydrazine and acetic acid in refluxing ethanol. Using Vilsmeier–Haack reaction conditions, these hydrazone derivatives were then reacted with POCl<sub>3</sub> and DMF resulting in 1,3-diarylpyrazoles (**3a**, **b**; **8**) with an aldehyde group at the 4 position. The 1-substituted phenyl-3-(pyridin-3/4-yl)-1*H*-pyrazole-4-carbaldehydes (**3a**, **b**; **8**) were then treated with malonic acid in pyridine to prepare the corresponding  $\alpha,\beta$ -unsaturated carboxylic acid derivatives (*2E*)-3-[1-phenyl-3-(pyridin-3/4-yl)-1*H*-pyrazol-4-yl]prop-2-enoic acids (**4a**, **b**; **9**), *via* the Knoevenagel condensation reaction. By treatment of **4a**, **b** and **9** with appropriate amines in the presence of DMAP and EDCI, which was used as the carboxylate activator, the resulting eighteen 3-[3-(pyrid-3-yl)-1-phenyl-1*H*-pyrazol-4-yl]acrylamide (**5a**–**s**) and nine 3-[3-(pyrid-4-yl)-1-phenyl-1*H*-pyrazol-4-yl]acrylamide (**10a**–**i**) derivatives were prepared in good yield (24–88%). The compounds were purified by automated flash chromatography and checked for purity with UPLC before being tested in biological assays (purity was >97%). The structures of these compounds were confirmed by high-resolution mass spectrometry (HRMS), IR, <sup>1</sup>H-NMR spectral data and elemental analysis. Detailed synthetic methods and analytical results for the obtained compounds are given in the Experimental section.

Structure–activity studies for the tricyclic class of selective COX-2 inhibitors have shown that a SO<sub>2</sub>Me or SO<sub>2</sub>NH<sub>2</sub> substituent at the *para* position of one aryl ring usually provides optimal COX-2 inhibitory potency.<sup>46</sup> The sulfonylmethyl COX-2 pharmacophore is a suitable scaffold to design COX-2 inhibitors and anti-cancer agents. Therefore, we aimed to introduce a sulfonylmethyl pharmacophore on the *para* position of the phenyl ring at position 1 of the pyrazole ring. In the 4-pyridyl derivatives of the synthesized compounds, the phenyl ring is located at position 1 of the pyrazole ring. During the synthesis studies, the pyrazole derivative bearing the sulfonylmethyl group at position 1 and the aldehyde functional group at position 4 cannot be obtained. Cyclization of some ketone hydrazones to 1-substituted 4-formylpyrazoles by using the Vilsmeier–Haack reagent (POCl<sub>3</sub>–DMF) involves double formylation and its mechanistic pathways are not certain. We obtained 4-(1-(4-(methylsulfonyl)phenyl)-1*H*-pyrazol-3-yl)pyridine **12** by the Vilsmeier–Haack reaction. Further

formylation of compound **12** was not achieved, consistent with the results of Kira *et al.*<sup>47</sup> Therefore, the synthesis of the amide derivatives intended to be obtained using this starting material has not been realized.



The C=O bands of the ketone carbonyl group of the starting compounds at 1675 cm<sup>-1</sup> were not observed in the IR spectrum of the synthesized hydrazone derivatives (**2a**, **b**; **7**). In the IR spectrum of the aldehyde derivatives (**3a**, **b**; **8**), the C=O stretching band of the aldehyde structure was observed at 1673, 1690 and 1669 cm<sup>-1</sup>, respectively. In the <sup>1</sup>H-NMR spectra of these compounds, the aldehyde proton was recorded at 10.06, 10.02 and 10.04 ppm, while the pyrazole ring proton was recorded at 8.58, 9.59 and 9.43 ppm, respectively. Compounds **2a**, **3a**, **4a**, **7**, **8** and **9** were previously reported.<sup>44</sup>

### Biological evaluations

**In vitro purified COX enzyme inhibition studies.** The COX-1 and COX-2 inhibitory activities of the compounds were examined by the EIA-COX inhibitor screening method (Cayman Chemical).<sup>48</sup> Preliminary screening of the inhibitory effects on the COX-1 and COX-2 isoforms of the compounds was carried out at a concentration of 10  $\mu$ M. Indomethacin (INDO) was used as the reference compound. The results are given in Table 1.

In the 3-pyridyl derivatives, the inhibitory activity against COX-1 and COX-2 isoenzymes was not observed for derivatives bearing a phenyl ring at position 1 of the pyrazole ring. Compounds **5f** and **5g** showed the highest inhibitory potency in this series of compounds. Compound **5f** has 4-pyridylmethylamine at the amide part and exhibited 11% and 15% inhibitory activity against COX-1 and COX-2, respectively. Compound **5g** bearing a 2-pyridylethylamine group in the amide portion similarly showed poor inhibitory activity against COX-1 and COX-2 isozymes (3% and 10%, respectively).

In the 3-pyridyl derivatives, derivatives **5j**–**5s** with 4-sulfonylmethylphenyl substitution at position 1 on the pyrazole ring exhibited stronger inhibitory effects on the COX-1 and COX-2 isoenzymes than their unsubstituted counterparts **5a**–**5i**. Derivatives having an imidazole moiety at the amide part (**5j**, **5k** and **5l**) have markedly enhanced inhibitory activity against both isoenzymes. In particular, compound **5j** presented a high activity against the COX-2 enzyme (65% inhibition). This compound also showed 40%

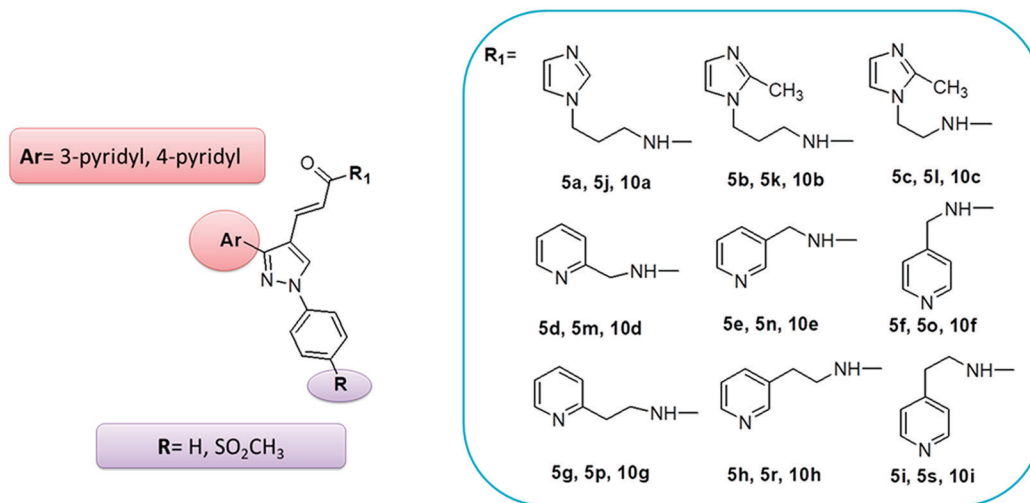


Fig. 2 Newly synthesized 1,3-diarylpyrazole derivatives.

inhibitory activity against the COX-1 enzyme. The highest inhibitory activity of compounds **5p** and **5s** was also observed among compounds (**5m**, **5n**, **5o**, **5p**, **5r** and **5s**) formed by conversion of cinnamic acid residues into the amide form with pyridylalkyl amine derivatives. These derivatives have a pyridylethylamine group at the amide part. Compounds bearing pyridylmethyl amine residues in the amide group are subject to a reduction in activity. Of these derivatives, only compound **5n** (having the pyrid-3-yl-methylamine group) had a potent inhibitory effect on COX-1 and COX-2 enzymes (58%).

In the 4-pyridyl derivatives, the phenyl ring is located at position 1 of the pyrazole ring. In these derivatives, only compound **10a** (possessing an imidazol-1-yl-propylamine residue) was found to be active against COX-1 and COX-2 enzymes (36%). Compounds carrying the pyridyl amine group in the amide moiety exhibit higher inhibitory activity against COX-1 and COX-2 enzymes when compared to those carrying the imidazole group. In particular, compounds **10d** (carrying the pyrid-2-yl-methylamine group) and **10g** (carrying the pyrid-2-yl-ethylamine group) had 43% and 49% inhibitory potency against the COX-2 enzyme, respectively. Compounds **10d** and **10g** showed weak inhibitory effects on the COX-1 enzyme.

### Inhibition of platelet aggregation

The antiplatelet effects of the compounds were tested at a final concentration of 100  $\mu$ M. As a reference, acetyl salicylic acid (ASA) was again used at the final concentration of 100  $\mu$ M. The activity results of AA and collagen-induced platelet aggregation are given in Tables 1 and 2.

As seen in Table 1, in the 3-pyridyl derivatives of the synthesized compounds, no inhibitory effect on the AA-induced platelet aggregation was found in the derivatives bearing a phenyl group (**5a–5i**) at position 1 of the pyrazole ring. However, these compounds were tested for collagen-induced platelet aggregation at the same concentration and the inhibitory effects on collagen-induced platelet aggregation were de-

termined. In particular, compounds **5a**, **5b**, **5d**, **5e**, **5h** and **5i** inhibited collagen-induced platelet aggregation in high percentages (86–56%).

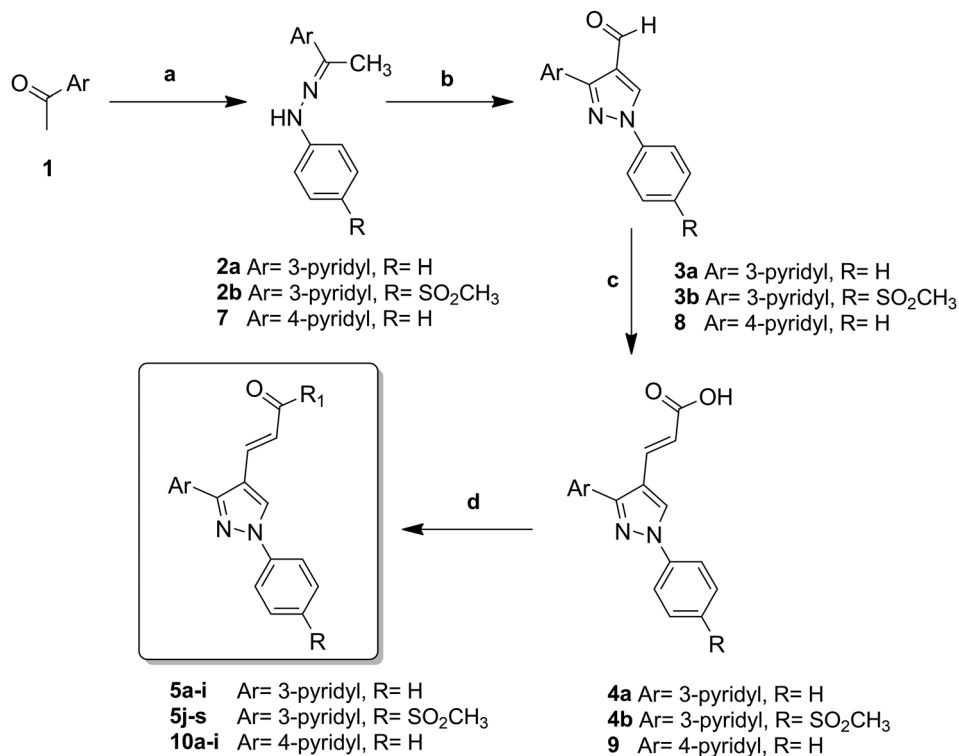
In the 3-pyridyl derivatives, the inhibitory effect on AA-induced platelet aggregation of the derivatives containing a sulfonylmethylphenyl ring at position 1 of the pyrazole ring markedly increased. Compounds **5j**, **5n**, **5p** and **5s** inhibited platelet aggregation induced by AA (82%, 89%, 90% and 100% inhibition, respectively). All of these derivatives were tested for collagen-induced platelet aggregation at the same concentration and were found to significantly inhibit collagen-induced platelet aggregation. Compound **5p** inhibited collagen-induced platelet aggregation by 78%.

In the 4-pyridyl derivatives, compounds **10a**, **10d**, **10g**, **10h** and **10i** strongly inhibited platelet aggregation induced by AA. Among them, compounds **10d** and **10g** inhibited AA-induced platelet aggregation at 100% percentage at 100  $\mu$ M concentration. These derivatives also showed an inhibitory effect on collagen-induced platelet aggregation. Compounds **10a**, **10h** and **10i** inhibited collagen-induced platelet aggregation by 88%, 86% and 74%, respectively.

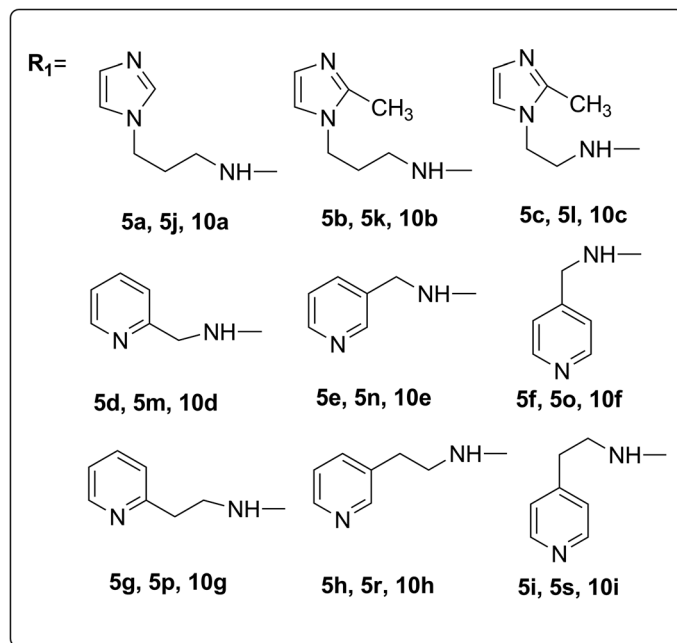
### Anticancer activity

The inducible COX-2 isoform is overexpressed in cancer tissues and is associated with critical events of tumorigenesis. COX-2 expression correlates with expression of angiogenic factors and new blood vessel formation. Inhibition of COX-2 favors apoptosis and causes a dose-dependent decline of tumor growth and metastasis.<sup>49</sup> Platelets play major roles in cancer progression.<sup>31,32</sup> Therefore, the anticancer potential of antiplatelet therapy has been intensively investigated for many years.<sup>33,34</sup> Advanced knowledge about the molecular and functional aspects of platelet-mediated tumor dissemination motivated scientists to search for drugs with anticancer potential.<sup>28</sup>

Towards this goal, we carried out a cytotoxic drug-screening method based on a sulforhodamine B assay (SRB)



**a)** Ph-NHNH<sub>2</sub> derivative, AcOH, EtOH **b)** DMF, POCl<sub>3</sub> **c)** Malonic acid, piperidine, pyridine  
**d)** RNH<sub>2</sub>, EDC, DMAP, DCM



**Scheme 1** Synthesis pathway to achieve the title compounds.

in triplicate to determine their IC<sub>50</sub> values<sup>50</sup> (Table 3). The cytotoxic activity of the synthesized compounds **5a–s** and **10a–i** was investigated on liver (Huh7), breast (MCF7) and colon (HCT116) cancer cell lines, by means of SRB assays in triplicate.

In general, compounds having a 3-pyridyl moiety at position 3 on the pyrazole ring (**5a–5i**) displayed moderate anti-proliferative potency on all cancer cell lines. Compounds having an imidazole moiety at the amide part of the molecules (**5a** and **5b**) showed good cytotoxicity with IC<sub>50</sub> values of

**Table 1** The *in vitro* inhibitory effects of the synthesized compounds on purified COX-1 and COX-2 enzymes and on platelet aggregation

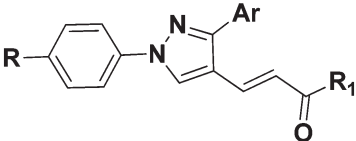
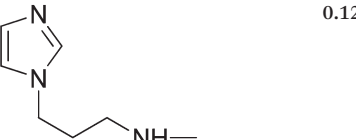
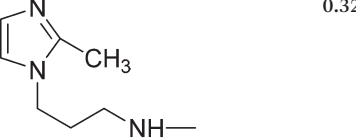
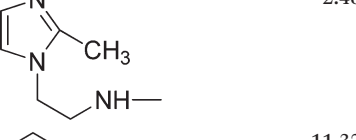
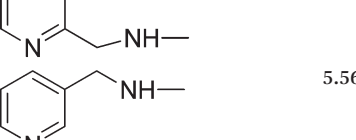
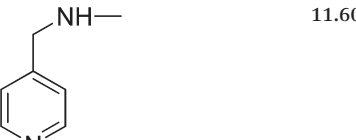
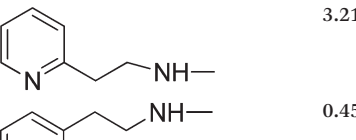
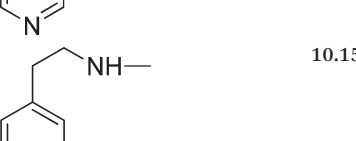

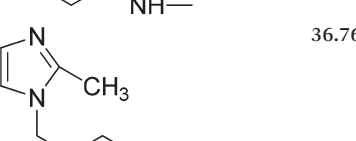
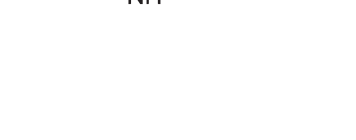
Comp.	Ar	R	R1	Inhibition %		Inhibition of platelet aggregation %	
				COX-1	COX-2	AA	Collagen
5a	3-Pyridyl	H		0.12	-30.52	16.14	86.52
5b	3-Pyridyl	H		0.32	11.17	1.24	60.26
5c	3-Pyridyl	H		2.46	2.55	0.0	15.52
5d	3-Pyridyl	H		11.32	-3.88	0.0	56.52
5e	3-Pyridyl	H		5.56	3.79	1.26	63.3
5f	3-Pyridyl	H		11.60	15.36	4.54	36.62
5g	3-Pyridyl	H		3.21	10.22	3.68	21.89
5h	3-Pyridyl	H		0.45	-5.65	0.0	76.59
5i	3-Pyridyl	H		10.15	-3.54	11.29	75.89
5j	3-Pyridyl	SO <sub>2</sub> CH <sub>3</sub>		40.55	65.16	82.40	52.65
5k	3-Pyridyl	SO <sub>2</sub> CH <sub>3</sub>		36.76	35.93	19.53	11.07

Table 1 (continued)

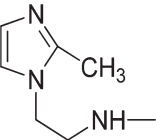
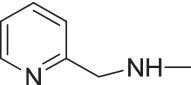
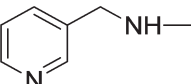
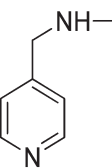
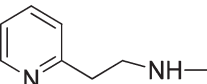
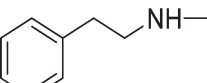
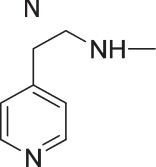
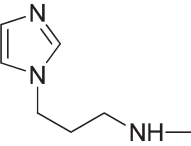
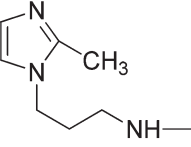
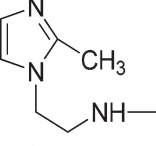
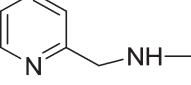
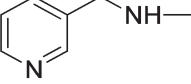
Comp.	Ar	R	R1	Inhibition %		Inhibition of platelet aggregation %	
				COX-1	COX-2	AA	Collagen
5l	3-Pyridyl	SO <sub>2</sub> CH <sub>3</sub>		29.57	36.92	14.3	8.60
5m	3-Pyridyl	SO <sub>2</sub> CH <sub>3</sub>		10.7	15.85	8.92	59.84
5n	3-Pyridyl	SO <sub>2</sub> CH <sub>3</sub>		13.1	58.85	89.98	64.11
5o	3-Pyridyl	SO <sub>2</sub> CH <sub>3</sub>		12.53	-29.64	6.20	40.87
5p	3-Pyridyl	SO <sub>2</sub> CH <sub>3</sub>		54.6	66.27	90.69	78.66
5r	3-Pyridyl	SO <sub>2</sub> CH <sub>3</sub>		1.31	5.43	14.55	70.26
5s	3-Pyridyl	SO <sub>2</sub> CH <sub>3</sub>		7.95	66.01	100	71.79
10a	4-Pyridyl	H		12.58	36.08	90.57	88.93
10b	4-Pyridyl	H		5.41	6.06	7.91	41.30
10c	4-Pyridyl	H		16.89	12.61	2.54	35.03
10d	4-Pyridyl	H		5.96	43.13	100	41.57
10e	4-Pyridyl	H		13.66	20.67	43.30	63.37

Table 1 (continued)

Comp.	Ar	R	R1	Inhibition %		Inhibition of platelet aggregation %	
				COX-1	COX-2	AA	Collagen
10f	4-Pyridyl	H		5.82	-2.74	4.96	50.09
10g	4-Pyridyl	H		13.06	49.67	100	41.87
10h	4-Pyridyl	H		9.37	16.27	93.67	86.90
10i	4-Pyridyl	H		26.55	25.45	71.43	74.58
INDO				69.52	84.27	—	—
ASA				—	—	100	100

13.4 and 14.3  $\mu\text{M}$  in the Huh7 cell line. These two derivatives had slight cytotoxicity ( $\text{IC}_{50} \sim 15.4\text{--}25.1 \mu\text{M}$ ) in the MCF7 and HCT116 cell lines. Compound 5c, bearing a short alkyl chain compared to other imidazole derivatives 5a and 5b, had weak activity for all cell lines used in this study ( $\text{IC}_{50} \sim 20.0\text{--}25.6 \mu\text{M}$ ). Compounds 5d–5h have 2-, 3- and 4-pyrimidine moieties at the amide part. Among these derivatives, 5h was the most active compound against the Huh7 cell line with an  $\text{IC}_{50}$  value of 8.1  $\mu\text{M}$ . 5h had decreased cytotoxicity against the MCF7 and HCT116 cancer cell lines.

Replacing the 3-pyridyl moiety (5a–5i) with a 4-pyridyl group (10a–10i), in general, resulted in a slight decrease in the cytotoxic activity of the compounds. Interestingly, the most active compounds among all synthesized derivatives belong to the 4-pyridyl series. Compounds 10a and 10i exhibited good cytotoxic activity especially against the Huh7 cell line ( $\text{IC}_{50} = 6.8$  and  $6.5 \mu\text{M}$ , respectively). Compound 10i was the most active derivative among all tested compounds

on the MCF7 and HCT116 cell lines with  $\text{IC}_{50}$  values of 11.0 and 7.1  $\mu\text{M}$ , respectively.

Introducing the 4-sulfonylmethyl group to phenyl at position 1 on the pyrazole ring (5j–5s) resulted in the loss of the cytotoxic activity of the compounds with the exception of derivatives 5m and 5s bearing a 2-pyrimidinylmethyl group and a 4-pyrimidinylethyl group at the amide part, respectively. Compounds 5m and 5s exhibited weak cytotoxic activity especially against Huh7 ( $\text{IC}_{50} = 24.7$  and  $38.7 \mu\text{M}$ , respectively) and HCT116 ( $\text{IC}_{50} = 27.0$  and  $19.8 \mu\text{M}$ , respectively).

### Lipinski's rule of five and drug-likeness profile

**Physicochemical properties of the synthesized compounds.** The synthesized compounds 5a–s and 10a–10i were submitted to an *in silico* evaluation using a molecular modeling approach. To predict the drug-like properties of the synthesized compounds, we analyzed these derivatives according to the rule-of-five developed by Lipinski *et al.*<sup>51</sup> Lipinski's 'rule-of-five' and the later addition of other parameters such as PSA<sup>52</sup> describe the molecular properties important for a drug's pharmacokinetics in the human body. PSA has been shown to be a very good descriptor characterizing drug absorption, including intestinal absorption, bioavailability, Caco-2 permeability and blood–brain barrier penetration.

Table 2  $\text{IC}_{50}$  ( $\mu\text{M}$ ) of the most active compounds on AA-induced platelet aggregation

Compound	5n	5p	5s	10a	10d	10g	10h	ASA
$\text{IC}_{50}$ ( $\mu\text{M}$ )	49.77	10.14	21.43	33.57	78.33	32.80	29.07	7.70



**Table 3** Cytotoxicity of compounds **5a–5s**, **10a–10i** and nucleoside analogue 5-FU assessed in different human cancer cells

Comp.	IC <sub>50</sub> <sup>a</sup> (μM)		
	Huh7	MCF7	HCT116
5a	14.3	15.4	17.6
5b	13.4	25.1	21.4
5c	25.6	21.8	20.0
5d	18.5	27.8	24.5
5e	21.0	30.9	21.6
5f	24.4	NI <sup>b</sup>	NI
5g	18.9	24.9	14.2
5h	8.1	30.8	16.9
5i	14.5	NI	26.7
5j	NI	NI	NI
5k	NI	NI	NI
5l	NI	NI	NI
5m	24.7	NI	27.0
5n	NI	NI	NI
5o	NI	NI	31.7
5p	NI	14.3	NI
5r	NI	NI	NI
5s	38.7	NI	19.8
10a	6.8	NI	18.5
10b	21.1	NI	10.8
10c	21.0	NI	12.6
10d	14.7	NI	20.4
10e	NI	NI	14.6
10f	32.6	NI	19.9
10g	27.3	12.2	NI
10h	NI	16.1	14.6
10i	6.5	11.0	7.1
5-FU	21.0	1.4	18.4

<sup>a</sup> Experiments were performed in triplicate and  $R^2$  values were between 1–0.8. <sup>b</sup> NI: no inhibition.

This approach has been widely used as a filter for substances that are likely to be further developed in drug design programs.  $\log P$ , the measure of a compound's solubility and permeability, is believed to be very important. Very high lipophilicity and the resulting large  $\log P$  values cause poor absorption or permeation and should be avoided.

Predictions of ADME properties for these compounds are given in Table 4. The calculated physicochemical properties<sup>53</sup> showed that all of the compounds fulfilled Lipinski's 'rule-of-five'. Theoretically, these compounds should present good passive oral absorption and differences in their bioactivity cannot be attributed to this property. However, introducing the 4-sulfonylethyl group to phenyl at position 1 on the pyrazole ring (**5j–5s**) resulted in very polar compounds ( $\log P$  values of 0.48–1.35). Compounds **5j**, **5k**, **5l**, **5m**, **5n** and **5o** had very low  $\log P$  values of 0.67, 0.75, 0.48, 0.94, 0.88 and 0.82, respectively, which might be disadvantageous with regard to the pharmacokinetic properties of these molecules in biological systems. These compounds were found inactive in cytotoxicity screening against all cell lines except **5m**, **5o**, **5p** and **5s** demonstrating weak activity. The rest of the compounds exhibited higher  $\log P$  values. Along with this, compounds **5h**, **10a** and **10i**, which showed good antitumor screening results (Huh7 cells, IC<sub>50</sub> = 8.1, 6.8 and 6.5 μM, re-

spectively), have optimal  $\log P$  values, compared to other compounds in the series. The total polar surface area (TPSA) was calculated based on the methodology published by Ertl *et al.*<sup>52</sup> as sums of O- and N-centered polar fragment contributions. The PSA is closely related to the hydrogen bonding potential of a compound. The TPSAs of the synthesized compounds were relatively small in comparison with the average value for acceptable drug molecules (<90 Å<sup>2</sup>) except for compounds **5j–5s** (TPSA = 106.85–111.78 Å<sup>2</sup>), which were found to be inactive in cytotoxicity screening as mentioned above. We were not able to find a direct correlation between the TPSA values and anti-inflammatory and antiplatelet activities of the tested compounds. However, it has to be kept in mind that  $\log P$  and PSA values are the two most important features, although not sufficient for predicting oral absorption of a drug.

**Drug-likeness and toxicity profile of compounds 5a–s and 10a–10i.** Currently, there are many approaches to assess a compound's drug-likeness based on topological descriptors, fingerprints of molecular drug-likeness structure keys.<sup>54</sup> In this work, we used the DataWarrior program<sup>55</sup> for calculating the physicochemical properties (solubility and drug-likeness) and the toxicity risks (mutagenicity, tumorigenicity, irritation and reproduction) of compounds **5a–s** and **10a–10i** (Table 4). The aqueous solubility of a compound significantly affects its absorption and distribution characteristics. Typically, a low solubility goes along with bad absorption and therefore, in general, the aim is to avoid poorly soluble compounds. More than 80% of the drugs on the market have a (estimated)  $\log S$  value of greater than  $-4$ . The  $\log S$  values of most of our compounds **5a–s** and **10a–10i** are around  $-3$ . Drug-likeness may be defined as a complex balance of various molecular properties and structural features which determine whether a particular molecule is similar to known drugs. These properties influence the behavior of a molecule in a living organism, including bioavailability, transport properties, affinity to proteins, reactivity, toxicity, metabolic stability and many others. It is interesting that most of our compounds demonstrated good drug-likeness values (from 6.10 to 2.57). A positive value states that the molecule contains predominantly fragments which are frequently present in commercial drugs. None of the compounds exhibited a toxic profile.

## Conclusion

In conclusion, we have designed and synthesized compounds that are potential inhibitors of cyclooxygenase and thromboxane synthase enzymes, which play an important role in the arachidonic acid pathway. The antiplatelet and anti-inflammatory activities of the synthesized compounds were investigated *in vitro*. The design of the compounds was made according to the work done in this area in the literature and the results of the preliminary tests obtained in our laboratory. The aim is to combine both COX and antiplatelet activities on the same compound. The synthesized compounds were designed as a tricyclic structure carrying a

**Table 4** Calculated physicochemical properties and the drug-likeness of the synthesized compounds

Compd.	Predicted oral bioavailability		M. W. <sup>c</sup>	clog P <sup>d</sup>	clog S <sup>e</sup>	TPSA <sup>f</sup>	Drug-likeness
	HBA <sup>a</sup>	HBD <sup>b</sup>					
5a	7	1	398.47	1.80	-2.39	77.64	5.04
5b	7	1	412.50	1.88	-2.02	77.64	4.36
5c	7	1	398.47	1.61	-1.75	77.64	4.73
5d	6	1	381.44	2.07	-3.26	72.71	2.74
5e	6	1	381.44	2.01	-3.23	72.71	2.74
5f	6	1	381.44	1.95	-3.23	72.71	2.74
5g	6	1	395.47	2.48	-3.37	72.71	2.83
5h	6	1	395.47	2.41	-3.34	72.71	2.83
5i	6	1	395.47	2.36	-3.34	72.71	2.83
5j	9	1	476.56	0.67	-2.81	111.78	6.10
5k	9	1	490.59	0.75	-2.43	111.78	5.52
5l	9	1	476.56	0.48	-2.16	111.78	5.82
5m	8	1	459.53	0.94	-3.67	106.85	4.13
5n	8	1	459.53	0.88	-3.65	106.85	3.97
5o	8	1	459.53	0.82	-3.23	106.85	2.74
5p	8	1	473.56	1.35	-3.79	106.85	4.26
5r	8	1	473.56	1.28	-3.76	106.85	4.09
5s	8	1	473.56	1.23	-3.76	106.85	2.57
10a	7	1	398.47	1.58	-2.39	77.64	5.04
10b	7	1	412.50	1.67	-2.02	77.64	4.36
10c	7	1	398.47	1.40	-1.75	77.64	4.73
10d	6	1	381.44	1.85	-3.26	72.71	2.74
10e	6	1	381.44	1.79	-3.23	72.71	2.74
10f	6	1	381.44	1.74	-3.23	72.71	2.74
10g	6	1	395.47	2.26	-3.37	72.71	2.83
10h	6	1	395.47	2.19	-3.34	72.71	2.83
10i	6	1	395.47	2.14	-3.34	72.71	2.83

<sup>a</sup> Number of hydrogen bond acceptors. <sup>b</sup> Number of hydrogen bond donors. <sup>c</sup> Molecular weight. <sup>d</sup> Calculated lipophilicity. <sup>e</sup> Solubility parameter. <sup>f</sup> Topological polar surface area (Å<sup>2</sup>).

nonsubstituted/*para*-methanesulfonyl-substituted phenyl ring at the 1 position of the central pyrazole ring, while having a 3/4-pyridyl group at the 3 position of the central pyrazole ring. Synthesis of the designed compounds and investigation of COX and antiplatelet effects revealed that compounds **5n**, **5p**, **5s**, **10d**, **10g** and **10i** were dual COX-2 inhibitor/antiplatelet compounds. Compound **10h** appeared to be a compound that exhibited antiplatelet activity without inhibiting the COX enzyme.

With the knowledge of the anticancer potential of COX-2 inhibitors and antiplatelet agents, we screened the anticancer activity of the synthesized compounds. Compounds **5h**, **10a** and **10i** were the most effective derivatives which displayed antiproliferative activity with IC<sub>50</sub> values smaller than 10 μM against hepatocellular (Huh7), breast (MCF7) and colon carcinoma (HCT116) cells. Maximal inhibitory effects were observed with these three compounds, in accord with their antiplatelet effects. Particularly, compound **10i**, as the compound exhibiting the highest anticancer, antiplatelet and COX-2 inhibitory activity, was remarkable.

The physicochemical properties of the synthesized compounds were also evaluated *in silico*, and it was found that some of our compounds should present good passive oral absorption. All synthesized compounds demonstrated good drug-likeness values. Thus, the results of this study have reached the conclusions that will form the basis of further

studies. In particular, further optimization studies can be planned as a result of the structure–activity relationships.

## Experimental

### Chemistry

Chemicals were purchased from commercial vendors and were used without purification. Thin-layer chromatography (TLC) was performed on Merck 60F254 plates. Reactions were monitored by TLC on silica gel, with detection by UV light (254 nm) or charring Dragendorff reagent.<sup>56</sup> Melting points were determined with an SMP-II digital melting point apparatus and are uncorrected (Schorpp Geraetetechnik, Germany). IR spectra were obtained in-house using a Perkin Elmer Spectrum 400 FTIR/FTNIR spectrometer equipped with a universal ATR sampling accessory. <sup>1</sup>H-NMR spectra were recorded in CDCl<sub>3</sub> or DMSO-*d*<sub>6</sub> on a Varian Mercury 400 MHz FT-NMR spectrometer using tetramethylsilane as the internal standard at the NMR facility of the Faculty of Pharmacy, Ankara University. All chemical shifts were recorded as δ (ppm). High-resolution mass spectral data (HRMS) were collected in-house using a Waters LCT Premier XE mass spectrometer (high-sensitivity orthogonal acceleration time-of-flight instrument) operating in ESI (+) mode also coupled to an ACQUITY ultra performance liquid chromatography system (Waters Corporation, Milford, MA, USA). Flash chromatography was

performed with a Combiflash® Rf automated flash chromatography system with RediSep columns (Teledyne-Isco, Lincoln, NE, USA) using dichloromethane–methanol solvent gradients.

***N*-(4-Methanesulfonylphenyl)-*N'*-(1-pyridin-3-yl-ethylidene)hydrazine (2b).** A solution of acetylpyridine derivative (0.052 mol), phenyl hydrazine derivative (0.058 mol) and acetic acid (2 ml, 0.035 mol) in ethanol was stirred for 2 h under reflux, and then evaporated. The precipitate was filtered off and dried. Yield 78%, mp 176.8–178 °C. IR (FTIR/FTNIR-ATR): 3299 cm<sup>-1</sup> (N–H), 2988 cm<sup>-1</sup> (aliphatic C–H). <sup>1</sup>H-NMR (DMSO-*d*<sub>6</sub>) δ: 10.04 (1H, s), 9.01 (1H, d, *J* = 2 Hz), 8.53 (1H, dd, *J*<sub>a</sub> = 1.6 Hz, *J*<sub>b</sub> = 4.8 Hz), 8.17 (1H, dt, *J*<sub>a</sub> = 1.6 Hz, *J*<sub>b</sub> = 7.6 Hz), 7.74 (2H, d, *J* = 9.2 Hz), 7.45–7.40 (3H, m), 3.12 (3H, s), 2.34 (3H, s). HRMS C<sub>14</sub>H<sub>16</sub>N<sub>3</sub>O<sub>2</sub>S [M + H]<sup>+</sup> calc. 290.0963, found *m/z* 290.0969. Anal. calc. (%) for C<sub>14</sub>H<sub>15</sub>N<sub>3</sub>O<sub>2</sub>S calc. % C: 58.11, H: 5.23, N: 14.52, S: 11.08, found % C: 58.02, H: 5.33, N: 14.38, S: 10.99.

**1-(4-Methanesulfonylphenyl)-3-(pyridin-3-yl)-1*H*-pyrazole-4-carbaldehyde (3b).** In a dry flask, phosphorochloride (POCl<sub>3</sub>) (0.124 mol) was added dropwise to an ice-cold stirred solution of hydrazone derivative (0.041 mol) in 80 ml DMF. The reaction mixture was allowed to attain room temperature, and then heated at 50 °C for 4 h. The resulting mixture was poured onto crushed ice, neutralized with dilute NaOH and left overnight. The yellow precipitate obtained was purified by crystallization in toluene. Yield 85%, mp 216.4–217 °C. IR (FTIR/FTNIR-ATR): 1690 cm<sup>-1</sup> (C=O). <sup>1</sup>H-NMR (DMSO-*d*<sub>6</sub>) δ: 10.02 (1H, s), 9.59 (1H, s), 9.12 (1H, d, *J* = 2 Hz), 8.70 (1H, dd, *J*<sub>a</sub> = 1.6 Hz, *J*<sub>b</sub> = 5.2 Hz), 8.35 (1H, dt, *J*<sub>a</sub> = 2 Hz, *J*<sub>b</sub> = 8 Hz), 8.30 (2H, d, *J* = 8.8 Hz), 8.14 (2H, d, *J* = 8.4 Hz), 7.58–7.55 (1H, m), 3.42 (3H, s). HRMS C<sub>16</sub>H<sub>14</sub>N<sub>3</sub>O<sub>3</sub>S [M + H]<sup>+</sup> calc. 328.0756, found *m/z* 328.0748. Anal. calc. (%) for C<sub>16</sub>H<sub>13</sub>N<sub>3</sub>O<sub>3</sub>S calc. % C: 58.70, H: 4.00, N: 12.84, S: 9.80, found % C: 58.98, H: 3.90, N: 12.86, S: 9.80.

**(2*E*)-3-[1-(4-Methanesulfonylphenyl)-3-(pyridin-3-yl)-1*H*-pyrazol-4-yl]acrylic acid (4b).** To a solution of 1-phenyl-3-(pyridin-3/4-yl)-1*H*-pyrazole-4-carbaldehyde (8.72 mmol) in pyridine (20 ml), malonic acid (0.035 mol) and piperidine (0.0131 mol) were added, and the reaction mixture was refluxed for 4 h. Upon cooling, the reaction mixture was poured onto a solution (100 ml) of crushed ice and concentrated HCl (50% by volume), then the pH was adjusted to 5. The resulting precipitate was filtered off, washed with acidified water and dried. Yield 97%, mp 316–318 °C. IR (FTIR/FTNIR-ATR): 1677 cm<sup>-1</sup> (C=O). <sup>1</sup>H-NMR (DMSO-*d*<sub>6</sub>) δ: 12.44 (1H, s), 9.45 (1H, s), 8.86 (1H, m), 8.72 (1H, m), 8.21 (2H, m), 8.14–8.07 (3H, m), 7.63–7.60 (1H, m), 7.47 (1H, d, *J* = 16 Hz), 6.49 (1H, d, *J* = 16 Hz), 3.25 (3H, s). HRMS C<sub>18</sub>H<sub>16</sub>N<sub>3</sub>O<sub>4</sub>S [M + H]<sup>+</sup> calc. 370.0862, found *m/z* 370.0852.

#### General procedure for the preparation of 3-(3-(pyrid-3/4-yl)-1-phenyl-1*H*-pyrazol-4-yl)acrylamide derivatives (5a–s and 10a–i)

To the solution of acid derivatives (0.692 mmol) in dichloromethane were added EDCI (0.761 mmol) and DMAP

(0.138 mmol). After addition of the appropriate amine derivatives (0.761 mmol), the mixture was stirred overnight. DCM was added, and the organic phase was washed with a 1% NaHCO<sub>3</sub> solution and brine, dried over Na<sub>2</sub>SO<sub>4</sub>, and evaporated under vacuum. The residue was purified by flash column chromatography (Combiflash® Rf) using DCM–MeOH as eluents.

**(2*E*)-*N*-(3-Imidazol-1-ylpropyl)-3-[1-phenyl-3-(pyridin-3-yl)-1*H*-pyrazol-4-yl]acrylamide (5a).** Elution with DCM–MeOH (0–10%) gave 5a as a white solid. Yield 48%, mp 116.5–118 °C. IR (FTIR/FTNIR-ATR): 1669 cm<sup>-1</sup> (C=O), 3249 cm<sup>-1</sup> (N–H). <sup>1</sup>H-NMR (CDCl<sub>3</sub>) δ: 8.95 (1H, d, *J* = 1.2 Hz), 8.65 (1H, m), 8.19 (1H, s), 7.99 (1H, dt, *J*<sub>a</sub> = 2 Hz, *J*<sub>b</sub> = 8 Hz), 7.75 (2H, d, *J* = 7.6 Hz), 7.62 (1H, d, *J* = 15.2 Hz), 7.52–7.48 (3H, m), 7.42–7.26 (2H, m), 7.06 (1H, s), 6.96 (1H, s), 6.18 (1H, d, *J* = 15.2 Hz), 5.87 (1H, t, *J* = 6 Hz), 4.03 (2H, t, *J* = 7 Hz), 3.38 (2H, q, *J* = 6.8 Hz), 2.06 (2H, m). HRMS C<sub>23</sub>H<sub>23</sub>N<sub>6</sub>O [M + H]<sup>+</sup> calc. 399.1933, found *m/z* 399.1915. Anal. calc. (%) for C<sub>23</sub>H<sub>22</sub>N<sub>6</sub>O calc. % C: 69.33, H: 5.57, N: 21.09, found % C: 69.13, H: 5.92, N: 21.23.

**(2*E*)-*N*-[3-(2-Methylimidazol-1-yl)propyl]-3-[1-phenyl-3-(pyridin-3-yl)-1*H*-pyrazol-4-yl]acrylamide (5b).** Elution with DCM–MeOH (0–20%) gave 5b as a white solid. Yield 30%, mp 153.2–154 °C. IR (FTIR/FTNIR-ATR): 1650 cm<sup>-1</sup> (C=O), 3281 cm<sup>-1</sup> (N–H). <sup>1</sup>H-NMR (DMSO-*d*<sub>6</sub>) δ: 9.05 (1H, s), 8.84 (1H, d, *J* = 2 Hz), 8.67 (1H, dd, *J*<sub>a</sub> = 1.6 Hz, *J*<sub>b</sub> = 4 Hz), 8.20 (1H, t, *J* = 5.6 Hz), 8.04 (1H, d, *J* = 2 Hz), 7.95 (2H, d, *J* = 8 Hz), 7.56 (3H, m), 7.39 (1H, t, *J* = 8 Hz), 7.37 (1H, d, *J* = 15.6 Hz), 7.07 (1H, s), 6.72 (1H, s), 6.49–6.45 (1H, d, *J* = 16 Hz), 3.88 (2H, t, *J* = 7 Hz), 3.16 (2H, q, *J* = 6.4 Hz), 2.26 (3H, s), 1.84 (2H, m). HRMS C<sub>24</sub>H<sub>25</sub>N<sub>6</sub>O [M + H]<sup>+</sup> calc. 413.2090, found *m/z* 413.2074. Anal. calc. (%) for C<sub>24</sub>H<sub>24</sub>N<sub>6</sub>O calc. % C: 69.88, H: 5.86, N: 20.37, found % C: 69.84, H: 5.82, N: 20.26.

**(2*E*)-*N*-[2-(2-Methylimidazol-1-yl)ethyl]-3-[1-phenyl-3-(pyridin-3-yl)-1*H*-pyrazol-4-yl]acrylamide (5c).** Elution with DCM–MeOH (0–20%) gave 5c as a white solid. Yield 24%, mp 123–124.8 °C. IR (FTIR/FTNIR-ATR): 1655 cm<sup>-1</sup> (C=O), 3139 cm<sup>-1</sup> (N–H). <sup>1</sup>H-NMR (DMSO-*d*<sub>6</sub>) δ: 9.06 (1H, s), 8.83 (1H, d, *J* = 1.6 Hz), 8.68 (1H, dd, *J*<sub>a</sub> = 1.6 Hz, *J*<sub>b</sub> = 4.4 Hz), 8.28 (1H, t, *J* = 2 Hz), 8.03 (1H, dt, *J*<sub>a</sub> = 2 Hz, *J*<sub>b</sub> = 8 Hz), 7.95 (2H, d, *J* = 8 Hz), 7.57 (3H, m), 7.40 (1H, m), 7.37 (1H, d, *J* = 15.6 Hz), 7.01 (1H, s), 6.72 (1H, s), 6.44 (1H, d, *J* = 16 Hz), 3.99 (2H, t, *J* = 6 Hz), 3.42 (2H, q, *J* = 6 Hz), 2.25 (3H, s). HRMS C<sub>23</sub>H<sub>23</sub>N<sub>6</sub>O [M + H]<sup>+</sup> calc. 399.1933, found *m/z* 399.1918. Anal. calc. (%) for C<sub>23</sub>H<sub>22</sub>N<sub>6</sub>O·0.45H<sub>2</sub>O calc. % C: 67.95, H: 5.68, N: 20.67, found % C: 68.09, H: 5.65, N: 20.40.

**(2*E*)-3-[1-Phenyl-3-(pyridin-3-yl)-1*H*-pyrazol-4-yl]-*N*-(pyridin-2-ylmethyl)acrylamide (5d).** Elution with DCM–MeOH (0–10%) gave 5d as a white solid. Yield 54%, mp 197–198 °C. IR (FTIR/FTNIR-ATR): 1650 cm<sup>-1</sup> (C=O), 3278 cm<sup>-1</sup> (N–H). <sup>1</sup>H-NMR (CDCl<sub>3</sub>) δ: 8.96 (1H, d, *J* = 1.6 Hz), 8.65 (1H, dd, *J*<sub>a</sub> = 1.6 Hz, *J*<sub>b</sub> = 4.4 Hz), 8.54 (1H, d, *J* = 4.4 Hz), 8.21 (1H, s), 7.97 (1H, t, *J* = 2 Hz), 7.75 (2H, d, *J* = 7.6 Hz), 7.66 (1H, d, *J* = 15.2 Hz), 7.65 (1H, m), 7.50 (2H, t, *J* = 7.6 Hz), 7.40–7.30 (3H, m), 7.23–7.20 (1H, m), 7.03 (1H, t, *J* = 4.8 Hz), 6.38 (1H, d, *J* = 15.2 Hz), 4.68 (2H, d, *J* = 5.2 Hz). HRMS C<sub>23</sub>H<sub>20</sub>N<sub>5</sub>O [M + H]<sup>+</sup>

calc. 382.1668, found  $m/z$  382.1656. Anal. calc. (%) for  $C_{23}H_{19}N_5O$  calc. % C: 72.42, H: 5.02, N: 18.36, found % C: 72.58, H: 5.27, N: 18.31.

(2*E*)-3-[1-Phenyl-3-(pyridin-3-yl)-1*H*-pyrazol-4-yl]-*N*-(pyridin-3-ylmethyl)acrylamide (5e). Elution with DCM–MeOH (0–10%) gave 5e as a white solid. Yield 55%, mp 197–198 °C. IR (FTIR/FTNIR-ATR): 1646  $cm^{-1}$  (C=O), 3275  $cm^{-1}$  (N–H).  $^1H$ -NMR ( $CDCl_3$ )  $\delta$ : 8.93 (1H, d,  $J = 1.6$  Hz), 8.62 (1H, dd,  $J_a = 1.6$  Hz,  $J_b = 4.4$  Hz), 8.53 (1H, d,  $J = 2$  Hz), 8.50 (1H, dd,  $J_a = 1.6$  Hz,  $J_b = 4.8$  Hz), 8.19 (1H, s), 7.97 (1H, dt,  $J_a = 2$  Hz,  $J_b = 8$  Hz), 7.74 (2H, d,  $J = 7.6$  Hz), 7.70–7.66 (2H, m), 7.49 (2H, t,  $J = 8$  Hz), 7.40–7.33 (2H, m), 7.28–7.25 (1H, m), 6.29 (1H, t,  $J = 6$  Hz), 6.25 (1H, d,  $J = 15.6$  Hz), 4.56 (2H, d,  $J = 6$  Hz). HRMS  $C_{23}H_{20}N_5O$   $[M + H]^+$  calc. 382.1668, found  $m/z$  382.1678. Anal. calc. (%) for  $C_{23}H_{19}N_5O$  calc. % C: 72.42, H: 5.02, N: 18.36, found % C: 72.10, H: 5.00, N: 18.10.

(2*E*)-3-[1-Phenyl-3-(pyridin-3-yl)-1*H*-pyrazol-4-yl]-*N*-(pyridin-4-ylmethyl)acrylamide (5f). Elution with DCM–MeOH (0–10%) gave 5f as a white solid. Yield 50%, mp 217–218 °C. IR (FTIR/FTNIR-ATR): 1649  $cm^{-1}$  (C=O), 3272  $cm^{-1}$  (N–H).  $^1H$ -NMR ( $CDCl_3$ )  $\delta$ : 8.94 (1H, d,  $J = 2$  Hz), 8.64 (1H, dd,  $J_a = 1.6$  Hz,  $J_b = 4.4$  Hz), 8.53 (2H, d,  $J = 6.4$  Hz), 8.21 (1H, s), 7.99 (1H, dt,  $J_a = 2$  Hz,  $J_b = 8$  Hz), 7.75 (2H, d,  $J = 7.6$  Hz), 7.70 (1H, d,  $J = 15.6$  Hz), 7.49 (2H, t,  $J = 7.8$  Hz), 7.41–7.36 (2H, m), 7.21 (2H, d,  $J = 6$  Hz), 6.28 (1H, d,  $J = 15.6$  Hz), 6.22 (1H, m), 4.56 (2H, d,  $J = 6.4$  Hz). HRMS  $C_{23}H_{20}N_5O$   $[M + H]^+$  calc. 382.1668, found  $m/z$  382.1676. Anal. calc. (%) for  $C_{23}H_{19}N_5O$  calc. % C: 72.42, H: 5.02, N: 18.36, found % C: 72.23, H: 5.32, N: 18.26.

(2*E*)-3-[1-Phenyl-3-(pyridin-3-yl)-1*H*-pyrazol-4-yl]-*N*-(2-pyridin-2-ylethyl)acrylamide (5g). Elution with DCM–MeOH (0–10%) gave 5g as a white solid. Yield 56%, mp 185–186.2 °C. IR (FTIR/FTNIR-ATR): 1669  $cm^{-1}$  (C=O), 3274  $cm^{-1}$  (N–H).  $^1H$ -NMR ( $CDCl_3$ )  $\delta$ : 8.97 (1H, d,  $J = 2$  Hz), 8.66 (1H, dd,  $J_a = 2$  Hz,  $J_b = 4.4$  Hz), 8.53 (1H, d,  $J = 4$  Hz), 8.20 (1H, s), 7.98 (1H, dt,  $J_a = 1.6$  Hz,  $J_b = 8$  Hz), 7.75 (2H, d,  $J = 8$  Hz), 7.64 (1H, m), 7.59 (1H, d,  $J = 15.2$  Hz), 7.49 (2H, t,  $J = 7.6$  Hz), 7.41–7.33 (2H, m), 7.20–7.15 (2H, m), 6.73 (1H, m), 6.23 (1H, d,  $J = 15.2$  Hz), 3.78 (2H, q,  $J = 6$  Hz), 3.04 (2H, t,  $J = 6.2$  Hz). HRMS  $C_{24}H_{22}N_5O$   $[M + H]^+$  calc. 396.1824, found  $m/z$  396.1806. Anal. calc. (%) for  $C_{24}H_{21}N_5O$  calc. % C: 72.89, H: 5.35, N: 17.71, found % C: 72.56, H: 5.52, N: 17.52.

(2*E*)-3-[1-Phenyl-3-(pyridin-3-yl)-1*H*-pyrazol-4-yl]-*N*-(2-pyridin-3-ylethyl)acrylamide (5h). Elution with DCM–MeOH (0–10%) gave 5h as a white solid. Yield 63%, mp 211–213 °C. IR (FTIR/FTNIR-ATR): 1649  $cm^{-1}$  (C=O), 3279  $cm^{-1}$  (N–H).  $^1H$ -NMR ( $DMSO-d_6$ )  $\delta$ : 9.04 (1H, s), 8.84 (1H, d,  $J = 1.6$  Hz), 8.68 (1H, dd,  $J_a = 1.6$  Hz,  $J_b = 4.4$  Hz), 8.44 (1H, d,  $J = 1.6$  Hz), 8.42 (1H, dd,  $J_a = 1.6$  Hz,  $J_b = 6.4$  Hz), 8.23 (1H, t,  $J = 5.6$  Hz), 8.04 (1H, dt,  $J_a = 2$  Hz,  $J_b = 8$  Hz), 7.95 (2H, d,  $J = 8$  Hz), 7.66–7.63 (1H, m), 7.60–7.54 (3H, m), 7.36 (1H, d,  $J = 15.6$  Hz), 7.40–7.30 (2H, m), 6.45 (1H, d,  $J = 15.6$  Hz), 3.43 (2H, q,  $J = 6.8$  Hz), 2.80 (2H, t,  $J = 7$  Hz). HRMS  $C_{24}H_{22}N_5O$   $[M + H]^+$  calc. 396.1824, found  $m/z$  396.1811. Anal. calc. (%) for  $C_{24}H_{21}N_5O$  calc. % C: 72.89, H: 5.35, N: 17.71, found % C: 73.24, H: 5.45, N: 17.59.

(2*E*)-3-[1-Phenyl-3-(pyridin-3-yl)-1*H*-pyrazol-4-yl]-*N*-(2-pyridin-4-ylethyl)acrylamide (5i). Elution with DCM–MeOH (0–10%) gave 5i as a white solid. Yield 58%, mp 182–184 °C. IR (FTIR/FTNIR-ATR): 1649  $cm^{-1}$  (C=O), 3282  $cm^{-1}$  (N–H).  $^1H$ -NMR ( $DMSO-d_6$ )  $\delta$ : 9.04 (1H, s), 8.83 (1H, d,  $J = 2$  Hz), 8.68 (1H, dd,  $J_a = 1.6$  Hz,  $J_b = 4.4$  Hz), 8.46 (2H, d,  $J = 5.6$  Hz), 8.22 (1H, t,  $J = 5.6$  Hz), 8.03 (1H, dt,  $J_a = 2$  Hz,  $J_b = 8$  Hz), 7.95 (2H, d,  $J = 8$  Hz), 7.60–7.54 (3H, m), 7.39 (1H, t,  $J = 7.2$  Hz), 7.36 (1H, d,  $J = 15.6$  Hz), 7.25 (2H, d,  $J = 6$  Hz), 6.44 (1H, d,  $J = 15.6$  Hz), 3.44 (2H, q,  $J = 6$  Hz), 2.80 (2H, m). HRMS  $C_{24}H_{22}N_5O$   $[M + H]^+$  calc. 396.1824, found  $m/z$  396.1806. Anal. calc. (%) for  $C_{24}H_{21}N_5O$  calc. % C: 72.89, H: 5.35, N: 17.71, found % C: 72.54, H: 5.46, N: 17.47.

(2*E*)-*N*-(3-Imidazol-1-ylpropyl)-3-[1-(4-methanesulfonylphenyl)-3-(pyridin-3-yl)-1*H*-pyrazol-4-yl]acrylamide (5j). Elution with DCM–MeOH (0–15%) gave 5j as a white solid. Yield 52%, mp 213–215 °C. IR (FTIR/FTNIR-ATR): 1649  $cm^{-1}$  (C=O), 3280  $cm^{-1}$  (N–H).  $^1H$ -NMR ( $DMSO-d_6$ )  $\delta$ : 9.23 (1H, s), 8.86 (1H, d,  $J = 2.4$  Hz), 8.70 (1H, dd,  $J_a = 1.6$  Hz,  $J_b = 5$  Hz), 8.26–8.22 (3H, m), 8.11 (2H, d,  $J = 7.2$  Hz), 8.07 (1H, dt,  $J_a = 2$  Hz,  $J_b = 8.4$  Hz), 7.64 (1H, s), 7.59 (1H, q,  $J = 4.4$  Hz), 7.37 (1H, d,  $J = 15.6$  Hz), 7.19 (1H, s), 6.89 (1H, s), 6.49 (1H, d,  $J = 15.6$  Hz), 3.98 (2H, t,  $J = 6.4$  Hz), 3.29 (3H, s), 3.12 (2H, q,  $J = 5.6$  Hz), 1.90–1.87 (2H, m). HRMS  $C_{24}H_{25}N_6O_3S$   $[M + H]^+$  calc. 477.1709, found  $m/z$  477.1704. Anal. calc. (%) for  $C_{24}H_{24}N_6O_3S$  calc. % C: 60.49, H: 5.08, N: 17.64, S: 6.73, found % C: 59.95, H: 5.24, N: 17.26, S: 6.63.

(2*E*)-3-[1-(4-Methanesulfonylphenyl)-3-(pyridin-3-yl)-1*H*-pyrazol-4-yl]-*N*-[3-(2-methylimidazol-1-yl)propyl]acrylamide (5k). Elution with DCM–MeOH (0–15%) gave 5k as a white solid. Yield 42%, mp 253–255 °C. IR (FTIR/FTNIR-ATR): 1649  $cm^{-1}$  (C=O), 3285  $cm^{-1}$  (N–H).  $^1H$ -NMR ( $DMSO-d_6$ )  $\delta$ : 9.24 (1H, s), 8.86 (1H, d,  $J = 1.6$  Hz), 8.71 (1H, dd,  $J_a = 1.6$  Hz,  $J_b = 5$  Hz), 8.27–8.22 (3H, m), 8.11 (2H, d,  $J = 8.8$  Hz), 8.07 (1H, dt,  $J_a = 2$  Hz,  $J_b = 8.4$  Hz), 7.61–7.58 (1H, m), 7.37 (1H, d,  $J = 15.6$  Hz), 7.08 (1H, d,  $J = 1.2$  Hz), 6.74 (1H, d,  $J = 1.2$  Hz), 6.49 (1H, d,  $J = 15.6$  Hz), 3.89 (2H, t,  $J = 7$  Hz), 3.29 (3H, s), 3.15 (2H, q,  $J = 6.4$  Hz), 2.26 (3H, s), 1.85 (2H, m). HRMS  $C_{25}H_{27}N_6O_3S$   $[M + H]^+$  calc. 491.1865, found  $m/z$  491.1847. Anal. calc. (%) for  $C_{25}H_{26}N_6O_3S \cdot 0.9H_2O$  calc. % C: 59.25, H: 5.53, N: 16.58, S: 6.33, found % C: 59.37, H: 5.4, N: 16.43, S: 6.17.

(2*E*)-3-[1-(4-Methanesulfonylphenyl)-3-(pyridin-3-yl)-1*H*-pyrazol-4-yl]-*N*-[2-(2-methylimidazol-1-yl)ethyl]acrylamide (5l). Elution with DCM–MeOH (0–15%) gave 5l as a white solid. Yield 74%, mp 165–168 °C. IR (FTIR/FTNIR-ATR): 1667  $cm^{-1}$  (C=O), 3306  $cm^{-1}$  (N–H).  $^1H$ -NMR ( $DMSO-d_6$ )  $\delta$ : 9.26 (1H, s), 8.84 (1H, d,  $J = 1.6$  Hz), 8.71 (1H, dd,  $J_a = 1.6$  Hz,  $J_b = 4.8$  Hz), 8.41 (1H, t,  $J = 5.8$  Hz), 8.23 (2H, d,  $J = 8.8$  Hz), 8.11 (2H, d,  $J = 8.8$  Hz), 8.06 (1H, dt,  $J_a = 1.8$  Hz,  $J_b = 8$  Hz), 7.61 (1H, m), 7.36 (1H, d,  $J = 15.6$  Hz), 7.30 (1H, d,  $J = 1.6$  Hz), 7.12 (1H, d,  $J = 1.6$  Hz), 6.46 (1H, d,  $J = 15.6$  Hz), 4.10 (2H, t,  $J = 5.8$ ), 3.52 (2H, t,  $J = 5.6$  Hz), 3.29 (3H, s), 2.41 (3H, s). HRMS  $C_{24}H_{25}N_6O_3S$   $[M + H]^+$  calc. 477.1709, found  $m/z$  477.170. Anal. calc. (%) for  $C_{24}H_{24}N_6O_3S \cdot 2.5H_2O$  calc. % C: 55.27, H: 5.6, N: 16.11, S: 6.15, found % C: 55.07, H: 5.29, N: 15.82, S: 6.06.

(2*E*)-3-[1-(4-Methanesulfonylphenyl)-3-(pyridin-3-yl)-1*H*-pyrazol-4-yl]-*N*-(pyridin-2-ylmethyl)acrylamide (**5m**). Elution with DCM–MeOH (0–10%) gave **5m** as a white solid. Yield 42%, mp 228–229 °C. IR (FTIR/FTNIR-ATR): 1655 cm<sup>-1</sup> (C=O), 3279 cm<sup>-1</sup> (N–H). <sup>1</sup>H-NMR (DMSO-*d*<sub>6</sub>) δ: 9.27 (1H, s), 8.87 (1H, d, *J* = 1.6 Hz), 8.78 (1H, t, *J* = 6 Hz), 8.70 (1H, dd, *J*<sub>a</sub> = 1.6 Hz, *J*<sub>b</sub> = 4.8 Hz), 8.50 (1H, d, *J* = 4.4 Hz), 8.24 (2H, d, *J* = 7.2 Hz), 8.11 (2H, d, *J* = 7.2 Hz), 8.08 (1H, dt, *J*<sub>a</sub> = 2.4 Hz, *J*<sub>b</sub> = 6 Hz), 7.77 (1H, td, *J*<sub>a</sub> = 2 Hz, *J*<sub>b</sub> = 7.6 Hz), 7.61–7.58 (1H, m), 7.42 (1H, d, *J* = 15.6 Hz), 7.31–7.26 (2H, m), 6.62 (1H, d, *J* = 16 Hz), 4.48 (2H, d, *J* = 6.4 Hz), 3.29 (3H, s). HRMS C<sub>24</sub>H<sub>22</sub>N<sub>5</sub>O<sub>3</sub>S [M + H]<sup>+</sup> calc. 460.1443, found *m/z* 460.1447. Anal. calc. (%) for C<sub>24</sub>H<sub>21</sub>N<sub>5</sub>O<sub>3</sub>S calc. % C: 62.73, H: 4.61, N: 15.24, S: 6.98, found % C: 62.58, H: 4.70, N: 15.07, S: 6.93.

(2*E*)-3-[1-(4-Methanesulfonylphenyl)-3-(pyridin-3-yl)-1*H*-pyrazol-4-yl]-*N*-(pyridin-3-ylmethyl)acrylamide (**5n**). Elution with DCM–MeOH (0–10%) gave **5n** as a white solid. Yield 63%, mp 225–226 °C. IR (FTIR/FTNIR-ATR): 1648 cm<sup>-1</sup> (C=O), 3280 cm<sup>-1</sup> (N–H). <sup>1</sup>H-NMR (DMSO-*d*<sub>6</sub>) δ: 9.21 (1H, s), 8.83 (1H, d, *J* = 2 Hz), 8.73 (1H, t, *J* = 6 Hz), 8.66 (1H, dd, *J*<sub>a</sub> = 1.6 Hz, *J*<sub>b</sub> = 5 Hz), 8.47 (1H, d, *J* = 2 Hz), 8.42 (1H, dd, *J*<sub>a</sub> = 2 Hz, *J*<sub>b</sub> = 4.6 Hz), 8.19 (2H, d, *J* = 7.2 Hz), 8.07 (2H, d, *J* = 7.2 Hz), 8.04 (1H, dt, *J*<sub>a</sub> = 2 Hz, *J*<sub>b</sub> = 7.6 Hz), 7.65 (1H, dt, *J*<sub>a</sub> = 1.6 Hz, *J*<sub>b</sub> = 8 Hz), 7.57–7.54 (1H, m), 7.38 (1H, d, *J* = 16 Hz), 7.34–7.31 (1H, m), 6.51 (1H, d, *J* = 16 Hz), 4.37 (2H, d, *J* = 6 Hz), 3.25 (3H, s). HRMS C<sub>24</sub>H<sub>22</sub>N<sub>5</sub>O<sub>3</sub>S [M + H]<sup>+</sup> calc. 460.1443, found *m/z* 460.1447. Anal. calc. (%) for C<sub>24</sub>H<sub>21</sub>N<sub>5</sub>O<sub>3</sub>S calc. % C: 62.73, H: 4.61, N: 15.24, S: 6.98, found % C: 62.72, H: 4.70, N: 15.12, S: 7.00.

(2*E*)-3-[1-(4-Methanesulfonylphenyl)-3-(pyridin-3-yl)-1*H*-pyrazol-4-yl]-*N*-(pyridin-4-ylmethyl)acrylamide (**5o**). Elution with DCM–MeOH (0–10%) gave **5o** as a white solid. Yield 50%, mp 265–266 °C. IR (FTIR/FTNIR-ATR): 1651 cm<sup>-1</sup> (C=O), 3279 cm<sup>-1</sup> (N–H). <sup>1</sup>H-NMR (DMSO-*d*<sub>6</sub>) δ: 9.28 (1H, s), 8.87 (1H, d, *J* = 1.6 Hz), 8.80 (1H, t, *J* = 6 Hz), 8.70 (1H, dd, *J*<sub>a</sub> = 1.6 Hz, *J*<sub>b</sub> = 5.2 Hz), 8.50 (2H, d, *J* = 6 Hz), 8.24 (2H, d, *J* = 7.2 Hz), 8.10 (2H, d, *J* = 7.2 Hz), 8.08 (1H, dt, *J*<sub>a</sub> = 2 Hz, *J*<sub>b</sub> = 8 Hz), 7.61–7.58 (1H, m), 7.43 (1H, d, *J* = 15.6 Hz), 7.26 (2H, d, *J* = 6 Hz), 6.59 (1H, d, *J* = 15.6 Hz), 4.41 (2H, d, *J* = 5.6 Hz), 3.29 (3H, s). HRMS C<sub>24</sub>H<sub>22</sub>N<sub>5</sub>O<sub>3</sub>S [M + H]<sup>+</sup> calc. 460.1443, found *m/z* 460.1440. Anal. calc. (%) for C<sub>24</sub>H<sub>21</sub>N<sub>5</sub>O<sub>3</sub>S calc. % C: 62.73, H: 4.61, N: 15.24, S: 6.98, found % C: 63.08, H: 4.63, N: 15.23, S: 7.04.

(2*E*)-3-[1-(4-Methanesulfonylphenyl)-3-(pyridin-3-yl)-1*H*-pyrazol-4-yl]-*N*-(2-pyridin-2-ylethyl)acrylamide (**5p**). Elution with DCM–MeOH (0–10%) gave **5p** as a white solid. Yield 61%, mp 237–238 °C. IR (FTIR/FTNIR-ATR): 1654 cm<sup>-1</sup> (C=O), 3280 cm<sup>-1</sup> (N–H). <sup>1</sup>H-NMR (DMSO-*d*<sub>6</sub>) δ: 9.22 (1H, s), 8.86 (1H, d, *J* = 1.2 Hz), 8.71 (1H, dd, *J*<sub>a</sub> = 1.6 Hz, *J*<sub>b</sub> = 4.8 Hz), 8.51 (1H, m), 8.24 (3H, m), 8.11–8.05 (3H, m), 7.73–7.68 (1H, m), 7.61–7.58 (1H, m), 7.35 (1H, d, *J* = 16 Hz), 7.27–7.21 (2H, m), 6.47 (1H, d, *J* = 15.6 Hz), 3.58 (2H, q, *J* = 6.8 Hz), 3.29 (3H, s), 2.93 (2H, t, *J* = 7.2 Hz). HRMS C<sub>25</sub>H<sub>24</sub>N<sub>5</sub>O<sub>3</sub>S [M + H]<sup>+</sup> calc. 474.1600, found *m/z* 474.1592. Anal. calc. (%) for C<sub>25</sub>H<sub>23</sub>N<sub>5</sub>O<sub>3</sub>S calc. % C: 63.41, H: 4.90, N: 14.79, S: 6.77, found % C: 63.33, H: 4.79, N: 14.67, S: 6.78.

(2*E*)-3-[1-(4-Methanesulfonylphenyl)-3-(pyridin-3-yl)-1*H*-pyrazol-4-yl]-*N*-(2-pyridin-3-ylethyl)acrylamide (**5r**). Elution with DCM–MeOH (0–10%) gave **5r** as a white solid. Yield 88%, mp 188–191 °C. IR (FTIR/FTNIR-ATR): 1652 cm<sup>-1</sup> (C=O), 3269 cm<sup>-1</sup> (N–H). <sup>1</sup>H-NMR (DMSO-*d*<sub>6</sub>) δ: 9.19 (1H, s), 8.82 (1H, d, *J* = 1.6 Hz), 8.67 (1H, dd, *J*<sub>a</sub> = 1.6 Hz, *J*<sub>b</sub> = 4.4 Hz), 8.41 (1H, d, *J* = 2 Hz), 8.39 (1H, dd, *J*<sub>a</sub> = 1.6 Hz, *J*<sub>b</sub> = 4.8 Hz), 8.24 (1H, t, *J* = 5.6 Hz), 8.19 (2H, d, *J* = 8.8 Hz), 8.06 (2H, d, *J* = 9.2 Hz), 8.03 (1H, dt, *J*<sub>a</sub> = 2 Hz, *J*<sub>b</sub> = 8 Hz), 7.63 (1H, dt, *J*<sub>a</sub> = 2 Hz, *J*<sub>b</sub> = 7.6 Hz), 7.58–7.54 (1H, m), 7.31 (1H, d, *J* = 15.6 Hz), 7.29 (1H, m), 6.43 (1H, d, *J* = 15.6 Hz), 3.38 (2H, q, *J* = 6.6 Hz), 3.25 (3H, s), 2.77 (2H, t, *J* = 6.8 Hz). HRMS C<sub>25</sub>H<sub>24</sub>N<sub>5</sub>O<sub>3</sub>S [M + H]<sup>+</sup> calc. 474.1600, found *m/z* 474.1578. Anal. calc. (%) for C<sub>25</sub>H<sub>23</sub>N<sub>5</sub>O<sub>3</sub>S·2.05H<sub>2</sub>O calc. % C: 58.82, H: 5.35, N: 13.72, S: 6.28, found % C: 59.23, H: 5.18, N: 13.51, S: 5.84.

(2*E*)-3-[1-(4-Methanesulfonylphenyl)-3-(pyridin-3-yl)-1*H*-pyrazol-4-yl]-*N*-(2-pyridin-4-ylethyl)acrylamide (**5s**). Elution with DCM–MeOH (0–10%) gave **5s** as a white solid. Yield 70%, mp 225–228 °C. IR (FTIR/FTNIR-ATR): 1653 cm<sup>-1</sup> (C=O), 3283 cm<sup>-1</sup> (N–H). <sup>1</sup>H-NMR (DMSO-*d*<sub>6</sub>) δ: 9.19 (1H, s), 8.82 (1H, d, *J* = 2 Hz), 8.67 (1H, dd, *J*<sub>a</sub> = 1.6 Hz, *J*<sub>b</sub> = 4.6 Hz), 8.43 (2H, d, *J* = 6.4 Hz), 8.23 (1H, m), 8.19 (2H, d, *J* = 8.8 Hz), 8.07 (2H, d, *J* = 9.2 Hz), 8.03 (1H, dt, *J*<sub>a</sub> = 2 Hz, *J*<sub>b</sub> = 8 Hz), 7.56 (1H, m), 7.31 (1H, d, *J* = 16 Hz), 7.22 (2H, d, *J* = 6 Hz), 6.42 (1H, d, *J* = 16 Hz), 3.41 (2H, q, *J* = 6.5 Hz), 3.25 (3H, s), 2.77 (2H, t, *J* = 7 Hz). HRMS C<sub>25</sub>H<sub>24</sub>N<sub>5</sub>O<sub>3</sub>S [M + H]<sup>+</sup> calc. 474.1600, found *m/z* 474.1590. Anal. calc. (%) for C<sub>25</sub>H<sub>23</sub>N<sub>5</sub>O<sub>3</sub>S calc. % C: 63.41, H: 4.90, N: 14.79, S: 6.77, found % C: 62.99, H: 4.75, N: 14.49, S: 6.68.

(2*E*)-*N*-(3-Imidazol-1-ylpropyl)-3-[1-phenyl-3-(pyridin-4-yl)-1*H*-pyrazol-4-yl]acrylamide (**10a**). Elution with DCM–MeOH (0–10%) gave **10a** as a white solid. Yield 54%, mp 176.2–177 °C. IR (FTIR/FTNIR-ATR): 1666 cm<sup>-1</sup> (C=O), 3220 cm<sup>-1</sup> (N–H). <sup>1</sup>H-NMR (DMSO-*d*<sub>6</sub>) δ: 9.05 (1H, s), 8.73 (2H, d, *J* = 6 Hz), 8.23 (1H, t, *J* = 5.6 Hz), 7.95 (2H, d, *J* = 8 Hz), 7.66 (3H, d, *J* = 6 Hz), 7.57 (2H, t, *J* = 8 Hz), 7.43 (1H, d, *J* = 16 Hz), 7.39 (1H, t, *J* = 7.2 Hz), 7.20 (1H, s), 6.90 (1H, s), 6.49 (1H, d, *J* = 15.6 Hz), 3.99 (2H, m), 3.16–3.11 (2H, m), 1.92–1.87 (2H, m). HRMS C<sub>23</sub>H<sub>23</sub>N<sub>6</sub>O [M + H]<sup>+</sup> calc. 399.1933, found *m/z* 399.1945. Anal. calc. (%) for C<sub>23</sub>H<sub>22</sub>N<sub>6</sub>O·1.1H<sub>2</sub>O calc. % C: 66.04, H: 5.83, N: 20.09, found % C: 66.27, H: 5.59, N: 19.75.

(2*E*)-*N*-[3-(2-Methylimidazol-1-yl)propyl]-3-[1-phenyl-3-(pyridin-4-yl)-1*H*-pyrazol-4-yl]acrylamide (**10b**). Elution with DCM–MeOH (0–10%) gave **10b** as a white solid. Yield 34%, mp 141–143 °C. IR (FTIR/FTNIR-ATR): 1665 cm<sup>-1</sup> (C=O), 3287 cm<sup>-1</sup> (N–H). <sup>1</sup>H-NMR (DMSO-*d*<sub>6</sub>) δ: 9.05 (1H, s), 8.73 (2H, d, *J* = 6 Hz), 8.24–8.21 (1H, m), 7.95 (2H, d, *J* = 7.6 Hz), 7.65 (2H, d, *J* = 6.4 Hz), 7.59–7.55 (2H, m), 7.43 (1H, d, *J* = 15.6 Hz), 7.39 (1H, t, *J* = 7.2 Hz), 7.07 (1H, d, *J* = 1.2 Hz), 6.72 (1H, d, *J* = 1.2 Hz), 6.49 (1H, d, *J* = 16 Hz), 3.90–3.87 (2H, m), 3.16 (2H, q, *J* = 6 Hz), 2.26 (3H, s), 1.86–1.83 (2H, m). HRMS C<sub>24</sub>H<sub>25</sub>N<sub>6</sub>O [M + H]<sup>+</sup> calc. 413.2090, found *m/z* 413.2079. Anal. calc. (%) for C<sub>24</sub>H<sub>24</sub>N<sub>6</sub>O·1.75H<sub>2</sub>O calc. % C: 64.92, H: 6.24, N: 18.93, found % C: 65.15, H: 6.3, N: 18.66.

(2*E*)-*N*-[2-(2-Methylimidazol-1-yl)ethyl]-3-[1-phenyl-3-(pyridin-4-yl)-1*H*-pyrazol-4-yl]acrylamide (**10c**). Elution with DCM–MeOH (0–10%) gave **10c** as a white solid. Yield 33%, mp 203.3–205 °C. IR (FTIR/FTNIR-ATR): 1667 cm<sup>-1</sup> (C=O), 3192 cm<sup>-1</sup> (N–H). <sup>1</sup>H-NMR (DMSO-*d*<sub>6</sub>) δ: 9.02 (1H, s), 8.70 (2H, d, *J* = 6.4 Hz), 8.28 (1H, t, *J* = 6 Hz), 7.91 (2H, d, *J* = 8 Hz), 7.61 (2H, d, *J* = 6 Hz), 7.55–7.51 (2H, m), 7.41 (1H, d, *J* = 16 Hz), 7.36 (1H, t, *J* = 7.6 Hz), 6.99 (1H, d, *J* = 1.6 Hz), 6.69 (1H, d, *J* = 1.2 Hz), 6.42 (1H, d, *J* = 15.6 Hz), 3.98–3.94 (2H, m), 3.41 (2H, q, *J* = 5.2 Hz), 2.23 (3H, s). HRMS C<sub>23</sub>H<sub>23</sub>N<sub>6</sub>O [M + H]<sup>+</sup> calc. 399.1933, found *m/z* 399.1944. Anal. calc. (%) for C<sub>23</sub>H<sub>22</sub>N<sub>6</sub>O·0.45H<sub>2</sub>O calc. % C: 67.95, H: 5.68, N: 20.67, found % C: 68.13, H: 5.53, N: 20.39.

(2*E*)-3-[1-Phenyl-3-(pyridin-4-yl)-1*H*-pyrazol-4-yl]-*N*-(pyridin-2-ylmethyl)acrylamide (**10d**). Elution with DCM–MeOH (0–10%) gave **10d** as a white solid. Yield 32%, mp 196–197 °C. IR (FTIR/FTNIR-ATR): 1650 cm<sup>-1</sup> (C=O), 3277 cm<sup>-1</sup> (N–H). <sup>1</sup>H-NMR (DMSO-*d*<sub>6</sub>) δ: 9.08 (1H, s), 8.77–8.72 (3H, m), 8.51 (1H, d, *J* = 1.6 Hz), 7.97 (2H, d, *J* = 5.6 Hz), 7.77 (1H, td, *J*<sub>a</sub> = 2 Hz, *J*<sub>b</sub> = 6 Hz), 7.66 (2H, d, *J* = 6.4 Hz), 7.57 (2H, t, *J* = 8 Hz), 7.50 (1H, d, *J* = 15.6 Hz), 7.42–7.39 (1H, m), 7.31–7.26 (2H, m), 6.62 (1H, d, *J* = 16 Hz), 4.48 (2H, d, *J* = 6 Hz). HRMS C<sub>23</sub>H<sub>20</sub>N<sub>5</sub>O [M + H]<sup>+</sup> calc. 382.1668, found *m/z* 382.1650. Anal. calc. (%) for C<sub>23</sub>H<sub>19</sub>N<sub>5</sub>O calc. % C: 72.42, H: 5.02, N: 18.36, found % C: 72.35, H: 5.08, N: 18.07.

(2*E*)-3-[1-Phenyl-3-(pyridin-4-yl)-1*H*-pyrazol-4-yl]-*N*-(pyridin-3-ylmethyl)acrylamide (**10e**). Elution with DCM–MeOH (0–10%) gave **10e** as a white solid. Yield 51%, mp 186.3–187 °C. IR (FTIR/FTNIR-ATR): 1649 cm<sup>-1</sup> (C=O), 3267 cm<sup>-1</sup> (N–H). <sup>1</sup>H-NMR (DMSO-*d*<sub>6</sub>) δ: 9.07 (1H, s), 8.72 (3H, m), 8.52 (1H, d, *J* = 2 Hz), 8.46 (1H, dd, *J*<sub>a</sub> = 1.6 Hz, *J*<sub>b</sub> = 4.8 Hz), 7.95 (2H, d, *J* = 8 Hz), 7.70–7.67 (1H, m), 7.66 (2H, d, *J* = 6.4 Hz), 7.59–7.55 (2H, m), 7.49 (1H, d, *J* = 15.6 Hz), 7.42–7.35 (2H, m), 6.55 (1H, d, *J* = 16 Hz), 4.41 (2H, d, *J* = 5.6 Hz). HRMS C<sub>23</sub>H<sub>20</sub>N<sub>5</sub>O [M + H]<sup>+</sup> calc. 382.1668, found *m/z* 382.1654. Anal. calc. (%) for C<sub>23</sub>H<sub>19</sub>N<sub>5</sub>O·0.6H<sub>2</sub>O calc. % C: 70.43, H: 5.19, N: 17.85, found % C: 70.61, H: 5.29, N: 17.71.

(2*E*)-3-[1-Phenyl-3-(pyridin-4-yl)-1*H*-pyrazol-4-yl]-*N*-(pyridin-4-ylmethyl)acrylamide (**10f**). Elution with DCM–MeOH (0–10%) gave **10f** as a white solid. Yield 41%, mp 186 °C. IR (FTIR/FTNIR-ATR): 1653 cm<sup>-1</sup> (C=O), 3278 cm<sup>-1</sup> (N–H). <sup>1</sup>H-NMR (DMSO-*d*<sub>6</sub>) δ: 9.10 (1H, s), 8.79–8.76 (1H, m), 8.73 (2H, d, *J* = 6 Hz), 8.50 (2H, d, *J* = 5.6 Hz), 7.95 (2H, d, *J* = 8 Hz), 7.66 (2H, d, *J* = 6 Hz), 7.59–7.55 (2H, m), 7.50 (1H, d, *J* = 16 Hz), 7.43–7.39 (1H, m), 7.27 (2H, d, *J* = 5.6 Hz), 6.57 (1H, d, *J* = 16 Hz), 4.41 (2H, d, *J* = 5.6 Hz). HRMS C<sub>23</sub>H<sub>20</sub>N<sub>5</sub>O [M + H]<sup>+</sup> calc. 382.1668, found *m/z* 382.1663. Anal. calc. (%) for C<sub>23</sub>H<sub>19</sub>N<sub>5</sub>O calc. % C: 72.42, H: 5.02, N: 18.36, found % C: 72.32, H: 5.16, N: 18.20.

(2*E*)-3-[1-Phenyl-3-(pyridin-4-yl)-1*H*-pyrazol-4-yl]-*N*-(2-pyridin-2-ylethyl)acrylamide (**10g**). Elution with DCM–MeOH (0–10%) gave **10g** as a white solid. Yield 48%, mp 200.4–202 °C. IR (FTIR/FTNIR-ATR): 1656 cm<sup>-1</sup> (C=O), 3289 cm<sup>-1</sup> (N–

H). <sup>1</sup>H-NMR (DMSO-*d*<sub>6</sub>) δ: 9.04 (1H, s), 8.73 (2H, d, *J* = 5.6 Hz), 8.50 (1H, d, *J* = 4.8 Hz), 8.25–8.22 (1H, m), 7.95 (2H, d, *J* = 8 Hz), 7.71 (1H, td, *J*<sub>a</sub> = 2 Hz, *J*<sub>b</sub> = 6 Hz), 7.65 (2H, d, *J* = 5.6 Hz), 7.58–7.54 (2H, m), 7.42 (1H, d, *J* = 15.6 Hz), 7.40 (1H, t, *J* = 8.4 Hz), 7.28–7.21 (2H, m), 6.47 (1H, d, *J* = 15.6 Hz), 3.53 (2H, q, *J* = 7.2 Hz), 2.93 (2H, t, *J* = 7.2 Hz). HRMS C<sub>24</sub>H<sub>22</sub>N<sub>5</sub>O [M + H]<sup>+</sup> calc. 396.1824, found *m/z* 396.1817. Anal. calc. (%) for C<sub>24</sub>H<sub>21</sub>N<sub>5</sub>O calc. % C: 72.89, H: 5.35, N: 17.71, found % C: 72.56, H: 5.34, N: 17.51.

(2*E*)-3-[1-Phenyl-3-(pyridin-4-yl)-1*H*-pyrazol-4-yl]-*N*-(2-pyridin-3-ylethyl)acrylamide (**10h**). Elution with DCM–MeOH (0–10%) gave **10h** as a white solid. Yield 58%, mp 171.5–173 °C. IR (FTIR/FTNIR-ATR): 1651 cm<sup>-1</sup> (C=O), 3297 cm<sup>-1</sup> (N–H). <sup>1</sup>H-NMR (DMSO-*d*<sub>6</sub>) δ: 9.04 (1H, s), 8.73 (2H, d, *J* = 6 Hz), 8.45–8.42 (2H, m), 8.25 (1H, m), 7.95 (2H, d, *J* = 7.6 Hz), 7.65 (2H, m), 7.56 (3H, t, *J* = 8 Hz), 7.42 (1H, d, *J* = 16 Hz), 7.42–7.38 (1H, m), 7.38–7.31 (1H, m), 6.46 (1H, d, *J* = 16 Hz), 3.45–3.40 (2H, m), 2.82–2.79 (2H, m). HRMS C<sub>24</sub>H<sub>22</sub>N<sub>5</sub>O [M + H]<sup>+</sup> calc. 396.1824, found *m/z* 396.1821. Anal. calc. (%) for C<sub>24</sub>H<sub>21</sub>N<sub>5</sub>O·0.25H<sub>2</sub>O calc. % C: 72.07, H: 5.42, N: 17.51, found % C: 72.29, H: 5.28, N: 17.28.

(2*E*)-3-[1-Phenyl-3-(pyridin-4-yl)-1*H*-pyrazol-4-yl]-*N*-(2-pyridin-4-ylethyl)acrylamide (**10i**). Elution with DCM–MeOH (0–10%) gave **10i** as a white solid. Yield 56%, mp 199.7–201 °C. IR (FTIR/FTNIR-ATR): 1652 cm<sup>-1</sup> (C=O), 3271 cm<sup>-1</sup> (N–H). <sup>1</sup>H-NMR (DMSO-*d*<sub>6</sub>) δ: 9.04 (1H, s), 8.73 (2H, d, *J* = 6 Hz), 8.47 (2H, d, *J* = 5.6 Hz), 8.25 (1H, t, *J* = 5.6 Hz), 7.95 (2H, d, *J* = 7.6 Hz), 7.64 (2H, d, *J* = 6 Hz), 7.56 (2H, t, *J* = 8 Hz), 7.42 (1H, d, *J* = 16 Hz), 7.40 (1H, t, *J* = 7.6 Hz), 7.26 (2H, d, *J* = 6 Hz), 6.46 (1H, d, *J* = 15.6 Hz), 3.45 (2H, q, *J* = 5.6 Hz), 2.83–2.79 (2H, m). HRMS C<sub>24</sub>H<sub>22</sub>N<sub>5</sub>O [M + H]<sup>+</sup> calc. 396.1824, found *m/z* 396.1837. Anal. calc. (%) for C<sub>24</sub>H<sub>21</sub>N<sub>5</sub>O·0.55H<sub>2</sub>O calc. % C: 71.11, H: 5.50, N: 17.28, found % C: 71.11, H: 5.40, N: 17.13.

## Biological studies

**Cyclooxygenase (COX-1 and COX-2) enzyme inhibition assay.** The inhibitory activities of the synthesized compounds on the COX-1 and COX-2 enzymes were determined by an enzyme immunoassay method (EIA) using EIA-COX activity screening kits (Cayman Chemical, No: 560101). In this method, recombinant sheep COX-1 and COX-2 enzymes were used, and the possible inhibitory activities of the compounds on both enzymes were determined by testing the inhibitory effects of these enzymes on the formation of PGE<sub>2</sub> from arachidonic acid. PGE<sub>2</sub> is the major source of arachidonic acid metabolism in many cells.

This experiment is based on competition of PGE<sub>2</sub> and the PGE<sub>2</sub>–acetylcholinesterase conjugate (PGE<sub>2</sub> tracer) to bind to PGE<sub>2</sub> monoclonal antibody, which is limited in the assay medium. While the concentration of the PGE<sub>2</sub>–acetylcholinesterase conjugate, designated as PGE<sub>2</sub> tracer in the assay, is constant, the amount of free PGE<sub>2</sub> is variable and that of the PGE<sub>2</sub> monoclonal antibody-bound PGE<sub>2</sub> is inversely

proportional to the amount of free PGE2 in the experimental environment. If the resulting antibody–PGE2 complex is bound to the “goat polyclonal anti-mouse IgG antibody” previously immobilized on the walls of the wells in microplates, then Ellman's reagent containing the substrate for acetylcholinesterase is added to the wells after microplate washing to remove unbound reagents. After Ellman's reagent is added, the resulting product (5-thio-2-nitrobenzoic acid) of the enzymatic reaction catalyzed by acetylcholine esterase is strongly yellow in color and is directly proportional to the PGE2 viewer attached to the color intensity wells. The intensity of the yellow color formed in the wells is determined spectrophotometrically from the absorbance at 412 nm and the amount of PGE2 present in the test medium during the incubation period is calculated.

Each compound was tested at a concentration of 10  $\mu\text{M}$  and the % inhibition of enzyme activity for each compound was calculated from the inhibitory effects on PGE2 that would result from COX-1 and COX-2 enzymes. The amount of PGE2 in the wells was calculated from the standard curve generated by 8 different known quantities of PGE2.

**Effect of compounds on platelet aggregation.** For platelet isolation, human blood was collected into citrate Vacutainer (TM) tubes and used within 3 hours. Platelet aggregation was determined by a turbidimetric method on the found aggregometer (APAC 4004) of the Biochemistry Department of the Faculty of Pharmacy of Gazi University.

All compounds were tested at a final concentration of 100  $\mu\text{M}$ . 1% DMSO was used as the carrier. As a reference compound, aspirin was used at a concentration of 100  $\mu\text{M}$ . All procedures on human subjects were performed in accordance with the Helsinki Declaration with the approval of Gazi University Clinical Research Ethics Committee (Decision no. 304/2011). All subjects included in the study signed informed consent upon explanation of the study.

**Preparation of platelet-rich plasma (PRP).** Freshly drawn venous human citrated blood (sodium citrate 3.2%, 1:9 v/v) from healthy subjects, who had not taken drugs with anti-platelet activity for 10 days, was centrifuged at 800 rpm for 10 min to obtain PRP. After separation, samples were centrifuged at 1500 rpm for 10 min to obtain PPP. Platelet count in PRP was adjusted to  $3.8 \times 10^5$  platelets per ml using PPP.

**Determination of platelet aggregation.** Platelet aggregation was measured by using an aggregometer (APACT 4004, LABiTec, Ahrensburg, Germany) according to the turbidimetric method described by Born *et al.*<sup>57</sup> The test compound (or the standard inhibitor, aspirin) was dissolved in DMSO. PRP was incubated at 37 °C with constant stirring at 1100 rpm and stimulated with arachidonic acid (AA, final concentration = 700  $\mu\text{M}$ ) or collagen (5  $\mu\text{g ml}^{-1}$ ). A 199  $\mu\text{l}$  sample of PRP was placed in the cuvette of the aggregometer and incubated for 5 min with 0.5  $\mu\text{l}$  of test compound (or standard inhibitor, or DMSO) before addition of 10  $\mu\text{l}$  AA. The changes in optical density were monitored for 3 min. All experiments were performed in triplicate. Inhibition of platelet aggregation was

expressed as percentage of inhibition using the following equation:

$$\% \text{Inhibition} = \left( 1 - \frac{\text{Maximum aggregation of compound treated PRP}}{\text{Maximum aggregation of DMSO treated PRP}} \right) \times 100$$

### Cytotoxic bioactivity

**Cell culture.** Hepatocellular (Huh7), breast cancer (MCF7) and colon cancer (HCT116) cell lines were grown in Dulbecco's modified Eagle's medium (DMEM) supplemented with 10% fetal bovine serum (Invitrogen GIBCO), 1% non-essential amino acids (GIBCO, Invitrogen) and 100 units per ml penicillin and streptomycin and cells were maintained at 37 °C in a humidified incubator under 5%  $\text{CO}_2$ .

**SRB assay.** Cells were plated in 96-well plates (2000–3000 cells per well) and grown for 24 hours at 37 °C. Then, they were treated with the compounds (dissolved in DMSO) in a concentration range of 40, 20, 10, 5 and 2.5  $\mu\text{M}$ . After 72 h, the cells were fixed with 10% (v/v) trichloroacetic acid (MERCK) and stained with SRB solution (50  $\mu\text{l}$  of a 0.4% (m/v) SRB in 1% acetic acid solution). For the removal of unbound SRB, the cells were washed with 1% acetic acid and left for air-drying. Protein-bound SRB was solubilized in 10 mM Tris-base and absorbance measurements (515 nm) were performed using a 96-well plate reader. Cells treated with DMSO alone were used as controls for the  $\text{IC}_{50}$  calculations.<sup>50</sup> All experiments were conducted in triplicate and  $R^2$  values were between 1–0.8.

### Lipinski's rule of five and drug-likeness profile

In order to explore the bioavailability of the synthesized derivatives, theoretical calculations were carried out to predict some physicochemical properties of the synthesized compounds. The bioavailability of the compounds was assessed using ADME (absorption, distribution, metabolism and elimination) prediction methods. In particular, we calculated the compliance of compounds to Lipinski's rule of five.<sup>51</sup> Lipinski's 'rule-of-five' and the later addition of other parameters such as polar surface area (PSA)<sup>52</sup> describe the molecular properties important for a drug's pharmacokinetics in the human body. This approach has been widely used as a filter for substances that would likely be further developed in drug design programs. Poor absorption and permeation are more likely to occur when there are more than 5 hydrogen-bond donors (HBD) or more than 10 hydrogen-bond acceptors (HBA), the molecular mass (MM) is greater than 500, or the  $\log P$  value ( $\text{clog} P$ ) is greater than 5. The topological polar surface area (TPSA) should be smaller than 90  $\text{\AA}^2$ .<sup>58</sup> Molecules violating more than one of these rules may have problems with bioavailability.

## Conflicts of interest

The authors declare no competing interest.

## Acknowledgements

We greatly acknowledge The Scientific and Technological Research Council of Turkey (TÜBİTAK) for financial support (Grant No. 110S284).

## References

- G. Coruzzi, N. Venturi and S. Spaggiari, *Acta Biomed.*, 2007, **78**, 96–110.
- J. van Ryn, G. Trummlitz and M. Pairet, *Curr. Med. Chem.*, 2000, **7**, 1145–1161.
- J. A. Mitchell and T. D. Warner, *Nat. Rev. Drug Discovery*, 2006, **5**, 75–86.
- G. A. Fitzgerald, *N. Engl. J. Med.*, 2004, **351**, 1709–1711.
- C. D. Funk and G. A. Fitzgerald, *J. Cardiovasc. Pharmacol.*, 2007, **50**, 470–479.
- R. S. Bresalier, R. S. Sandler, H. Quan, J. A. Bolognese, B. Oxenius, K. Horgan, C. Lines, R. Riddell, D. Morton, A. Lanas, M. A. Konstam and J. A. Baron, *N. Engl. J. Med.*, 2005, **352**, 1092–1102.
- S. D. Solomon, J. J. V. McMurray, M. A. Pfeffer, J. Wittes, R. Fowler, P. Finn, W. F. Anderson, A. Zauber, E. Hawk and M. Bertagnolli, *N. Engl. J. Med.*, 2005, **352**, 1071–1080.
- P. McGettigan and D. Henry, *JAMA, J. Am. Med. Assoc.*, 2006, **296**, 1633–1644.
- M. Hamberg, J. Svensson and B. Samuelsson, *Proc. Natl. Acad. Sci. U. S. A.*, 1975, **72**, 2994–2998.
- S. Moncada and J. R. Vane, *Pharmacol. Rev.*, 1978, **30**, 293.
- X. De Leval, J. Hanson, J. L. David, B. Masereel, B. Pirotte and J. M. Dogne, *Curr. Med. Chem.*, 2004, **11**, 1243–1252.
- F. Krotz, T. M. Schiele, V. Klauss and H.-Y. Sohn, *J. Vasc. Res.*, 2005, **42**, 312–324.
- A. D. Michelson, *Nat. Rev. Drug Discovery*, 2010, **9**, 154–169.
- Xd. Leval, F. Julemont, J. Delarge, B. Pirotte and J. M. Dogne, *Curr. Med. Chem.*, 2002, **9**, 941–962.
- C. Michaux and C. Charlier, *Mini-Rev. Med. Chem.*, 2004, **4**, 603–615.
- A. L. Blobaum and L. J. Marnett, *J. Med. Chem.*, 2007, **50**, 1425–1441.
- G. Dannhardt and S. Laufer, *Curr. Med. Chem.*, 2000, **7**, 1101–1112.
- T. D. Penning, J. J. Talley, S. R. Bertenshaw, J. S. Carter, P. W. Collins, S. Docter, M. J. Graneto, L. F. Lee, J. W. Malecha, J. M. Miyashiro, R. S. Rogers, D. J. Rogier, S. S. Yu, G. D. Anderson, E. G. Burton, J. N. Cogburn, S. A. Gregory, C. M. Koboldt, W. E. Perkins, K. Seibert, A. W. Veenhuizen, Y. Y. Zhang and P. C. Isakson, *J. Med. Chem.*, 1997, **40**, 1347–1365.
- P. Prasit, Z. Wang, C. Brideau, C. C. Chan, S. Charleson, W. Cromlish, D. Ethier, J. F. Evans, A. W. Ford-Hutchinson, J. Y. Gauthier, R. Gordon, J. Guay, M. Gresser, S. Kargman, B. Kennedy, Y. Leblanc, S. Leger, J. Mancini, G. P. O'Neill, M. Ouellet, M. D. Percival, H. Perrier, D. Riendeau, I. Rodger and R. Zamboni, *Bioorg. Med. Chem. Lett.*, 1999, **9**, 1773–1778.
- Z. Sui, J. Guan, M. P. Ferro, K. McCoy, M. P. Wachter, W. V. Murray, M. Singer, M. Steber, D. M. Ritchie and D. C. Argentieri, *Bioorg. Med. Chem. Lett.*, 2000, **10**, 601–604.
- H. H. Kim, J. G. Park, T. C. Moon, H. W. Chang and Y. Jahng, *Arch. Pharmacol. Res.*, 1999, **22**, 372–379.
- K. Lizuka, K. Akahane, D. Momose and M. Nakazawa, *J. Med. Chem.*, 1981, **24**, 1139–1148.
- T. Tanouchi, M. Kawamura, I. Ohyama, I. Kajiwara, Y. Iguchi, T. Okada, T. Miyamoto, K. Taniguchi, M. Hayashi, K. Lizuka and M. Nakazawa, *J. Med. Chem.*, 1981, **24**, 1149–1155.
- G. Chan, J. O. Boyle, E. K. Yang, F. Zhang, P. G. Sacks, J. P. Shah, D. Edelstein, R. A. Soslow, A. T. Koki, B. M. Woerner, J. L. Masferrer and A. J. Dannenberg, *Cancer Res.*, 1999, **59**, 991–994.
- D. Hwang, J. Byrne, D. Schollard and E. Levine, *J. Natl. Cancer Inst.*, 1998, **90**, 455–460.
- H. Achiwa, Y. Yatabe, T. Hida, T. Kuroishi, K. Kozaki, S. Nakamura, M. Ogawa, T. Sugiura, T. Mitsudomi and T. Takahashi, *Clin. Cancer Res.*, 1999, **5**, 1001–1005.
- H. Wolff, K. Saukkonen, S. Anttila, A. Karjalainen, H. Vainio and A. Ristimäki, *Cancer Res.*, 1998, **58**, 4997–5001.
- M. Z. Wojtukiewicz, D. Hempel, E. Sierko, S. C. Tucker and K. V. Honn, *Cancer Metastasis Rev.*, 2017, **36**, 305–329.
- S. L. Fu, Y. L. Wu, Y. P. Zhang, M. M. Qiao and Y. Chen, *World J. Gastroenterol.*, 2004, **10**, 1971–1974.
- B. Liu, L. Qu and S. Yan, *Cancer Cell Int.*, 2015, **15**, 106.
- D. G. Menter, S. C. Tucker, S. Kopetz, A. K. Sood, J. D. Crissman and K. V. Honn, *Cancer Metastasis Rev.*, 2014, **33**, 231–269.
- M. Z. Wojtukiewicz, D. Hempel, E. Sierko, S. C. Tucker and K. V. Honn, *Cancer Metastasis Rev.*, 2016, **35**, 213–233.
- H. Sakai, T. Suzuki, Y. Takahashi, M. Ukai, K. Tauchi, T. Fujii, N. Horikawa, T. Minamimura, Y. Tabuchi, M. Morii, K. Tsukada and N. Takeg, *FEBS Lett.*, 2006, **580**, 3368–3374.
- D. Nie, M. Che, A. Zacharek, Y. Qiao, L. Li, X. Li, M. Lamberti, K. Tang, Y. Cai, Y. Guo, D. Grignon and K. V. Honn, *Am. J. Pathol.*, 2004, **6**, 429–439.
- E. Banoglu, M. Sukuroglu, B. C. Ergun, S. N. Baytas, E. Aypar and M. Ark, *Turk. J. Chem.*, 2007, **31**, 677–687.
- S. Unlu, S. N. Baytas, E. Kupeli and E. Yesilada, *Archiv. Pharm. Pharm. Med. Chem.*, 2003, **336**, 310–321.
- S. Nacak, D. S. Dogruer and M. F. Sahin, *Farmaco*, 1999, **54**, 768–772.
- S. N. Baytas, N. Inceler, A. Yilmaz, A. Olgac, S. Menevse, E. Banoglu, E. Hamel, R. Bortolozzi and G. Viola, *Bioorg. Med. Chem.*, 2014, **22**, 3096–3104.
- S. Ersan, S. Nacak, N. Noyanalpan and E. Yeşilada, *Arzneim. Forsch.*, 1997, **47**, 834–836.
- S. Baytas, N. Inceler, K. F. Mavaneh, M. O. Uludağ, N. Abacıoğlu and M. Gökçe, *Turk. J. Chem.*, 2012, **36**, 734–748.
- S. Baytas, N. N. T. Dural, Y. Özkan, H. B. Simsek, T. Gürsel and S. Ünlü, *Turk. J. Chem.*, 2012, **36**, 367–382.



- 42 S. Baytas, N. Inceler, Y. Ozkan, S. Unlu and M. F. Sahin, *Med. Chem. Res.*, 2013, **22**, 5922–5933.
- 43 N. Inceler, A. Yilmaz and S. N. Baytas, *Med. Chem. Res.*, 2013, **22**, 3109–3118.
- 44 S. N. Baytas, N. Inceler and A. Yilmaz, *Med. Chem. Res.*, 2013, **22**, 4893–4908.
- 45 M. M. A. Hawash, D. C. Kahraman, F. Eren, R. Cetin-Atalay and S. N. Baytas, *Eur. J. Med. Chem.*, 2017, **129**, 12–26.
- 46 I. K. Khanna, R. M. Weier, Y. Yu, X. D. Xu, F. J. Koszyk, P. W. Collins, C. M. Koboldt, A. W. Veenhuizen, W. E. Perkins, J. J. Casler, J. L. Masferrer, Y. Y. Zhang, S. A. Gregory, K. Seibert and P. C. Isakson, *J. Med. Chem.*, 1997, **40**, 1634–1647.
- 47 M. A. Kira, M. O. Abdel-Rahman and K. Z. Gadalla, *Tetrahedron Lett.*, 1969, **10**, 109–110.
- 48 P. Pradelles, J. Grassi and J. Maclouf, *Anal. Chem.*, 1985, **57**, 1170–1177.
- 49 J. Stoehlmacher and H. J. Lenz, *Semin. Oncol.*, 2003, **30**, 10–16.
- 50 A. Monks, D. Scudiero, P. Skehan, R. Shoemaker, K. Paull, D. Vistica, C. Hose, J. Langley, P. Cronise, A. Vaigro-Wolff, M. Gray-Goodrich, H. Campbell, J. Mayo and M. Boyd, *J. Natl. Cancer Inst.*, 1991, **83**, 757–766.
- 51 C. A. Lipinski, F. Lombardo, B. W. Dominy and P. J. Feeney, *Adv. Drug Delivery Rev.*, 2001, **46**, 3–26.
- 52 P. Ertl, B. Rohde and P. Selzer, *J. Med. Chem.*, 2000, **43**, 3714–3717.
- 53 <http://www.molinspiration.com>.
- 54 I. V. Tetko, *Drug Discovery Today*, 2005, **10**, 1497–1500.
- 55 <http://www.openmolecules.org>.
- 56 E. Stahl, *Thin-layer Chromatography*, Springer, New York, 1969.
- 57 G. V. Born and M. J. Cross, *J. Physiol.*, 1963, **168**, 178–195.
- 58 R. W. Brueggemeier, J. C. Hackett and E. S. Diaz-Cruz, *Endocr. Rev.*, 2005, **26**, 331–345.